Road Vehicle Recognition and Classification Using Magnetic Field Measurement

Xiao Chen

Faculty of Engineering and Information Technology

University of Technology Sydney

A thesis submitted for the degree of

Master of Research

June 2018

Certificate of Original Authorship

I certify that the work in this thesis has not previously been submitted for a degree nor has it been submitted as part of requirements for a degree except as fully acknowledged within the text.

I also certify that the thesis has been written by me. Any help that I have received in my research work and the preparation of the thesis itself has been acknowledged. In addition, I certify that all information sources and literature used are indicated in the thesis.

Student: Xiao CHEN

Date: 25/05/2018

Production Note:
Signature removed
prior to publication.

Acknowledgments

I benefited greatly and learned a wealth of methods and information from my advisor. Firstly, I would like to express my deepest gratitude to my principal supervisor Min Xu and co-supervisor Xiaoying Kong for providing me with such an excellent research environment. I am so lucky to have had my supervisor Min Xu as my professional mentor and academic advisor, as she provided excellent opportunities to help me explore academic research. Discussing any problems with her was always a humbling but rich experience, and she consistently gave me sufficient freedom to reflect and explore. Without her scientific expertise, endless patience and constant guidance, I would hardly have been able to accomplish my research. I am deeply appreciative of her support and advice.

In addition, I would especially like to express my deepest appreciation to my co-supervisor Xiaoying Kong. Her guidance and rigorous approach to all academic areas has been a great advantage and has inspired me to attain significant academic achievements in a short period of time. She taught me how to apply an academic method and rigorous style to my research area. All of this will certainly benefit my future research career.

My warm thanks to all members, visitors and students at the School of Electrical and Data Engineering, University of Technology, Sydney. Their helpful discussion and encouragement still inspire me.

I would like to dedicate this thesis to my family. They have always believed in me, continued to encourage me, given me indispensable suggestions, and fully supported all my decisions.

Finally, I would like to express my gratitude to both the Graduate School and the Faculty of Engineering and Information Technology, University of Technology, Sydney.

Table of Contents

Table of Figures

Table of Tables

Abstract

This dissertation presents a road vehicle detection approach for intelligent transportation systems. This approach uses a roadside-installed, low-cost magnetic sensor and associated data collection system. The system measures magnetic field changes to count, detect, and classify passing vehicles into a number of vehicle types. We compare each vehicle using dynamic time warping (DTW), then extend Mel-Frequency Cepstral Coefficients to analyse the vehicles' magnetic signals and extract them as vehicle features using the representations of cepstrum, frame energy, and gap cepstrum of magnetic signals. There are three directions (X-axis, Y-axis, and Z-axis directions) in the earth's magnetic field. We design one- (X-axis direction) and three-dimensional (i.e. X-axis, Y-axis, and Z-axis direction) map algorithms using Vector Quantisation to classify the vehicle magnetic features according to four typical vehicle types for the Australian suburbs: sedan, van, truck, and bus. We also compared experimental results between these two methods. Results show that our approach achieves a high level of accuracy for vehicle detection and classification. In the end, we found that filtering raw magnetic measurement signals can significantly influence vehicle recognition accuracy. Compared with the one-dimensional map, we reached the highest accuracy of vehicle classification in our test data using the three-dimensional map.

Keywords: signal processing, vehicle classification, road traffic model, intelligence vehicle, magnetic sensing

Chapter 1: Introduction

1.1. Introduction

Intelligent transportation systems (ITS) deploy sensors to collect and analyse road vehicle information for road vehicle monitoring, management, control of road traffic, and data analysis for future development of transportation infrastructure. Road traffic information includes passing vehicle location, vehicle type, vehicle speed and direction, vehicle weight, and vehicle volume in certain zones [1, 2]. The first traffic monitor sensor was developed and installed for road use in 1928. This device used a microphone to detect the sound of vehicles [1]. Since then, road vehicle sensing technologies have explored vibration, inductive-loop detection, magnetic fields, acoustic sensing, optical and infrared sensing, satellite signal processing, camera image and video processing, and inertial sensing [1, 2]. Sensing technologies can be utilised via a single sensor or a sensor network. Different types of sensing technologies can be applied at different locations in transportation systems. The sensors can be statically deployed at the roadside, underneath the road surface, over the road, on a pole at a certain height near the road, on a bridge crossing over a road, or dynamically installed in road or aerial vehicles. In a sensor network, these technologies and deployment locations can be integrated. From a commercial deployment perspective, the types of sensing technologies and the deployment locations of sensors will impact the benefits and costs of installation and maintenance. For example, magnetic sensor installation underneath the road surface will increase sensor measurement accuracy but disrupt road traffic in the installation and maintenance phases.

Among these sensing technologies, magnetic field sensing to analyse road vehicle information is at the exploration stage. Large-scale commercial deployment of magnetic sensors in intelligent transportation systems is not yet possible. There is a need to research magnetic sensing to detect, identify, and classify road vehicles from both a theoretical and quality evaluation perspective. Consequently, in this thesis, we present a road vehicle identification and classification approach using a roadside-installed single magnetic sensor. The magnetic sensor measures the magnetic field changes when vehicles pass by. The sensor measurement signals are then analysed to extract vehicle features, and these

features are classified into vehicle types. Four major types of passing vehicles in road traffic are therefore detected: sedan, van, truck and bus. From a deployment perspective, the magnetic sensing and detection approach does not require road traffic interruption for installation and maintenance and can be applied in day and night conditions. On the detection algorithm side, there are three directions, namely X, Y and Z, in the Earth's magnetic field. Therefore, we design one-dimensional (X-axis direction) and three-dimensional (i.e. X-axis, Y-axis, and Z-axis direction) approaches for the feature extraction and classification process. The experimental results validate this approach. This approach can be applied to intelligent transportation systems to provide dynamic information about road vehicle types and traffic flow conditions.

1.2 Background

Sensing technologies provide vehicle and road traffic information to intelligent transportation systems. An accelerometer is able to measure the vibration of the road when a vehicle is passing. An Intelligent transportation systems (ITS) can receive sensor input from accelerometers installed under the road surface and compute both the weight of a passing vehicle and the total number of vehicles. Inductive loop technology involves an electrical conducting loop being installed on the road surface. When a vehicle passes over the loop, current is induced in the wired loops, and this signal change is transmitted to the ITS to compute the detection of the passing vehicle type [1]. The vehicle detection and type classification algorithms include back-propagation neural networks [3], neural genetic controllers using a single loop [4, 5], and two-axle tractor/three-axle semi-trailer approaches [5, 6, 7]. Radar is a mature technology used to detect passing vehicle length, height and speed. Frequency-modulated continuous waves using doppler radar is one of the traditional radar techniques employed to extract shape information and classify vehicle types [8, 9]. More recent radar techniques include detection and analysis of the frequency of incoming vehicles using reconfigurable antenna arrays and the Synthetic Aperture Radar technique for estimation of angular coordinates [10]. Infrared (IR), including active infrared laser radar and passive infrared, has been used in road vehicle acquisition, tracking, and night vision. Infrared is capable of operating over multiple lanes [1, 11, 12]. IR detecting techniques include extracting histograms of oriented gradient features and local binary pattern features, which are concatenated to form classification

features [13, 14]. IR techniques can be applied to detect both vehicles and pedestrians on the road. Infrared sensors may exhibit reduced sensitivity to vehicles in weather conditions like rain, fog and snow [15]. Finally, cameras capture passing vehicles' location, speed and shape as images and videos. Road traffic images contain rich information about a wide area. Vehicle imaging detection techniques can be used across multiple lanes and multiple zones. Weather conditions and day-to-night transition may affect performance [16]. Street lighting is required to assist video image recording at night to ensure a reliable signal [17, 18].

In light of the above, and considering the cost of installation and maintenance, we opt to use a single anisotropic magneto-resistive (AMR) magnetic sensor to install at the roadside. When compared with other types of magnetic field sensing technologies on range and cost, AMR sensors are able to work in the range of magnetic field changes required for practical application [19]. Our approach is applied in an Australian road environment.

1.3 Motivations and objectives

Existing methods apply different types of sensors data to detect and/or classify vehicles. In the present research, our goal is to propose a vehicle detection and classification solution that can achieve satisfactory accuracy in vehicle classification and be robust to various environments, e.g. different weather conditions. The aim of this thesis is to concept proof the research idea of passing vehicles in low and high speed detection, raw magnetic data processing, vehicle feature extraction and build up an initial prototype which is not yet used in practice.

Considering that AMR sensors record magnetic signals in a stable fashion that is not influenced by weather conditions, in this research, we apply AMR sensors to collect raw data and further classify vehicle types based on these data.

In order to achieve the abovementioned goal, we tackle the following three research objectives:

- **Data collection**

In this thesis, an AMR sensor is deployed at a certain roadside position to detect passing vehicles. We collect the magnetic raw data as well as data pertaining to the vehicle types (as discussed in chapter 3).

- **Vehicle classification**

In order to classify vehicle types, we propose to treat the magnetic raw data as a signal, then apply signal processing techniques to extract features efficiently and select an effective classification algorithm. In our research, four main vehicle types are considered for classification: sedan, van, truck and bus.

- **Accuracy improvement**

To ensure satisfactory classification accuracy, we explore how different directions of magnetic data (i.e. the X-axis, Y-axis, and Z-axis directions) affect classification results. We compare the classification results of using a one-dimensional (X-axis direction) map and a three-dimensional (X-axis, Y-axis, and Z-axis directions) map in order to increase the accuracy of vehicle classification.

1.4 Thesis contributions

The contributions of this thesis are summarised as follows:

- In a departure from most existing methods, we utilise a single AMR magnetic sensor installed at roadside, which can provide a cost-efficient solution for road vehicle detection and classification, compared to other sensors, e.g. camera sensors, radar sensors and Infrared sensors.
- Treating magnetic data as a signal, we extract Mel-Frequency Cepstral Coefficients (MFCC) and apply Vector Quantisation (VQ) for classification. To ensure the training data are representative, Dynamic Time Warping (DTW) is applied for pre-processing.
- By applying different directions of magnetic data, i.e. the one-dimensional map and three-dimensional map, we have achieved satisfactory vehicle classification accuracy. Experimental results demonstrate that the three-dimensional map outperforms the one-dimensional map.

In the following, advantages of the proposed approach are highlighted as follows, compared the existing works using AMR sensors, our advantages are listed as below:

- On vehicle detection aspect, we consider the comprehensive passing vehicle situation, such as high speed, low speed and none-vehicle passing the sensor.
- On vehicle raw magnetic data aspect, we apply not only X-axis direction but also the combination of X-axis, Y-axis, and Z-axis directions as our data set.
- On raw magnetic data processing aspect, the effective magmatic data can be selected through the algorithm measuring similarity between signals as our training data set.
- On vehicle feature extraction aspect, the audio processing is used in magnetic field. The magnetic signal feature can be extracted through audio algorithm due to the similar physical characteristic.

1.5 Structure of the dissertation

This thesis is organised as follows. Chapter 1 reviews related work in vehicle recognition and introduces the approach of the present research. Chapter 2 presents different sensors used in detecting vehicles, while Chapter 3 discusses the collection of raw magnetic data. Chapters 4 and 5 compare the one-dimensional and three-dimensional algorithms to inform the experimental design for magnetic sensing in this research. The results of the road vehicle identification and classification are demonstrated and evaluated in Chapter 6. Finally, conclusions and suggestions for future work are presented in Chapter 7.

Chapter 2: Literature review

2.1 Vehicle recognition using different sensors

Previous work has employed different types of sensors, such as radar, infrared, camera, magnetic and so on, to perform vehicle measurement. Vehicles are detected using various sensors, and a vehicle's parameters (length, height and width dimensions, etc.) are extracted from images; these features are then used to classify vehicle types [20]. While many of these sensors detect different signal waves, images and frequencies, magnetic sensors measure the magnetic field. Types of magnetic sensing technologies include squid, fibre-optic, optical pumped, nuclear procession, search-coil, anisotropic magneto-resistive, flux-gate, etc. [21, 22, 23]. The impact of a vehicle passing or stopping on the Earth's magnetic field change is within the range of 1 microgauss to 10 gauss [24].

The various types of sensors will be introduced below. Ultimately, we opt to use the AMR sensor as our tool to detect and collect the vehicle data in this thesis.

2.1.1 Radar sensor

The major types of radar detection can be broadly divided into two types: microwave (MW) radar and millimetre wave (mmW) sensors. Firstly, in mmW sensors, the feature is electromagnetic (EM) backscattering fields from the target, and the echo signals are received by the radar system. Vehicle recognition can be performed well using the incident beams. Due to the metal structures being relative with EM scattering, the major contribution will result from the vehicle's side-front part. The below analysis of research involving two vehicles will present information regarding the effectiveness of radar in vehicle detection. In [25], operational frequency is set at 24.125 GHz. The distances between the antennas and vehicles are 4.7m, simulating the side-looking radar detection scenario, which results in beam cross-sections with areas of 1.33 and 0.5 metres respectively. The positions of the antennas relative to the vehicles are varied horizontally to simulate the scenario of a moving vehicle, while the vertical location of the antenna remains fixed at 2.55m. In the experiment, the narrow beam interacts with only a small portion of the vehicles and causes false detections [26, 27]. Subsequently, the AMASM

method is applied to smooth out the patterns of backscattering fields, which could effectively reduce the possibility of false detection and recognition [28].

Moreover, the microwave (MW) radars need to satisfy certain requirements. Firstly, the radiation pattern requires wide road coverage transverse to traffic flow and narrow coverage along the traffic flow. In addition, high distance resolution and sampling frequency are used to ensure the signals satisfy this requirement. Lastly, a wide dynamic range is provided according to the return amplitudes [29]. The feature vector comes from the sensor output as well as mapping it onto predefined classes. Feature vector extraction, which can be defined as a linear metrical P-dimension vector, is the single-valued transformation of samples into feature vectors [30]. In terms of classification, the technique involves: calculating vehicle height, obtaining a feature vector, computing distances, finding indexes, and vehicle class estimation [31]. The main methods are observation and the proposed technique, which includes calculating the vector and estimation and termination algorithms.

2.1.2 Infrared (IR) sensor

Infrared systems for vehicle detection incorporate paired transmitter (Tx) and receiver (Rx) arrays that are mounted horizontally and vertically [32]. When a vehicle travels across the Tx and Rx towers, raw data is transformed into information regarding blockage of the infrared sensors for that certain timer. All these similar pulse cycles collectively produce a vehicle profile that is useful for vehicle counting and categorisation [33]. IR LED drivers may take the form of a transistorised switching circuit, which can transmit the train of pulses at an individual level in synchronisation with the Rx controller. The output of the IR sensor is connected to a controller that can read the particular sensor output at that IR LED. The vehicle profile generator will then receive raw data from the output IR LED and create the graphical vehicle profile. Vehicle classification is based on the processing of multiple combinations of the extracted data. In vehicle classification, the classification rule can be defined as valve selection, and the output identifies three kinds of vehicles, namely buses, trucks and cars. In [34], the detection of vehicles is accomplished using passive infrared temperature measurements and Gaussian Mixture Models (GMM) to classify the data (the speed and length of vehicles are estimated by the GMM algorithm). However, the average performance results, which are at around 80%

accuracy, are not at the level of high precision we expect; moreover, a limited number of vehicles were used in the experiment. In [35], a low-cost infrared-based system is used for vehicle classification. The system has two parts: the emitter, which is responsible for emitting pulsed infrared light through LEDs, and the receiver, which is responsible for detecting the light reflected from a vehicle. The author uses Dynamic Time Warping (DTW) as a comparison tool in this case. For classification, the distance between two time series and the distance is to measure and to evaluate the similarity between two time series. If distance is null, the similarity is maximum and the vehicle type is the same; if not, it is a different kind of vehicle. Vehicles can be categorised with reference to this distance. Although this is a type of low-cost infrared-based system for vehicle classification, there is an environmental limitation, namely light condition. We need a stable and continuous system for vehicle classification.

2.1.3 Camera sensor

Cameras sensors utilise multiple cameras. In [36], each camera first extracts one image patch per vehicle, which is deemed a vehicle patch. Then, taking colour information into consideration, features are extracted based on Harris corner detection with Opponent SIFT descriptors. A Spatiotemporal Successive Dynamic Programming (S2DP) algorithm for multiple cameras is put forward to identify vehicles. The features are obtained from the patches from each camera and transferred into feature vectors. For performance evaluation and comparison, there are four approaches used in implementation and testing: firstly, the proposed S2DP algorithm, then the proposed S2DP algorithm without the consideration of the penalty A for non-successive assignment, followed by the baseline Hungarian algorithm [37, 38], and lastly the state-of-the-art approach proposed by Cabrera et al. The average accuracy S2DP's performance on vehicles is below 75%, and this paper only detected the presence of vehicles rather than classifying the different types of vehicles [39].

In [40], there are two videos used: one for training data, and the other for test data. The training data set includes 69 vehicles, including 20 cars, 44 motorcycles, and five tricycles; the other includes one car, five motorcycles, and one tricycle. A comparison is carried out between classification results using the back-propagation and Radial Basis Function

Network (RBFN) before and after applying Affine Transformation (AF). The highest result accuracy is 86% and 71%, respectively, which is after AF.

2.1.4 AMR sensor

When compared with other types of magnetic field sensing technologies on range and cost, Anisotropic Magneto-Resistive (AMR) sensors are best able to work in the range of magnetic field changes required for practical application [24]. As discussed, there are environmental limitations to the above sensors, such as rain or foggy weather; under these circumstances, the performance will be dramatically influenced and the accuracy will decrease. The magnetic field change measurements of AMR sensors used in road experiments have been analysed using vehicle detection and classification approaches. Signal analysis of magnetic field measurement and classification into signal shape patterns has proven to be an effective approach.

Compared with different types of sensors, such as radar, infrared, camera, magnetic and so on, AMR sensor has three main advantages:

- The AMR is the overall systems low cost and smaller size due to high sensitivity, and they still maintain reliability and quality.
- AMR sensors have high sensitivity and flexibility, therefore they are placed further away from the magnet. This allows the AMR sensor to be installed where it is needed for the optimal performance.
- The most advantage of these solid-state devices are their durability and immunity to shock and vibration. They record magnetic signals in a stable fashion that is not influenced by different weather conditions.

2.2 AMR sensor data

2.2.1 Sensor installation

The traditional geomagnetic detector for collecting traffic measurement data is placed at the roadside or at the centre of lanes, which provides a limited sample dataset. Therefore, it can only analyse the vehicle motion states and cannot fully extrapolate to real-time traffic conditions [41, 42]. By contrast, an anisotropic magneto-resistive (AMR) sensor deployed along travel lane markings can synthesise information from the three (X, Y, Z) axes to collect vehicle driving information from two adjacent lanes [43]. In addition, this method uses a single sensor node rather than double nodes to realise the detection of traffic flow parameters, and also increases accuracy as well as reducing installation and maintenance costs [44].

Our AMR sensor is mounted at the roadside. The distance between passing vehicles and the road is about 60cm. The road experiment is configured as shown in Figure 1. Axis-Y of the sensor is pointing to the direction of traffic flow, parallel to the roadside; Axis-X is pointing to the vehicle, vertical relative to Axis-Y; finally, Axis-Z is pointing up. The AMR sensor outputs three measurements as Mag-X, Mag-Y and Mag-Z. The unit of the sensor measurement in our experiment is the microgauss (mgauss). The magnetic field measurement is in the time domain. The passing vehicle types and vehicle passing time period are recorded. The collected measurement data are then used offline to analyse the types of vehicles. Further information on the identification and classification of vehicles is presented in the next section.

2.2.2 Sensor data collection

The Earth's magnetic field intensity is between 0.05–0.06 mT on average [45]. If there is no other disturbance, the magnetic field is constant. When the vehicle passes the magnetic field, the field's distribution will change [46]. AMR sensors use the anisotropic magneto-resistive effect of conductor materials. The resistance of the nickel-iron magnetic alloy has a function that is related to the angle (θ) between the bias current (I) and magnetic field vector (M) [47]; the passing vehicle changes the magnetic field vector.

In Meng Liu et al.'s approach [48], this AMR has a high sensitivity and triggers a response from a small disturbance, thus detecting the changes in the geomagnetic field. This

approach places the AMR sensor on the single lane line. The X-axis of the AMR sensor is defined as the direction opposite to the driving direction, the Y-axis as the horizontal component perpendicular to the driving direction, and the Z-axis as the vertical component perpendicular to the X-axis and the Y-axis [49].

2.2.3 Sensor data analytics

In Sing Yiu et al.'s approach [50], three-axis magnetic vectors are analysed separately in terms of magnitude. The magnitudes of Axis X, Y and Z in time series are classified into a number of patterns; these patterns illustrate the shape of hills for each vehicle type. Using this hill pattern approach, Saowaluck et al. [51] extracted features of normalised vehicle magnetic length, average energy, and number of peaks in hill patterns. Their classification types include motorcycles, cars, pickups, vans, and buses. An integrated approach was developed using two magnetic sensors and DGPS by Taghvaeeym and Rajamani [52]. DGPS measures the vehicle speed to aid the magnetic sensing. Vehicle classification is based on magnetic length and an estimate of the average vertical magnetic height of the vehicle. Vehicle length is computed using the vehicle presence time and vehicle speed. Moreover, using a single AMR sensor, Yang and Lei [53] detected vehicles in a single lane using sensor measurements when vehicles passed the road sensing area. AMR sensors can be installed at the roadside, under the road surface, using a single sensor, or using multiple sensors as a sensor network. These various configurations impact the factors of measured signal strength for detecting accuracy, cost of installation and maintenance. Application has not yet been commercialised at a large scale due to these impact factors. Consequently, further research into these approaches is needed in order to consider the commercial impact.

AMR sensor detection and measurement involves extracting the following features from measured signals for classification: signal duration, signal energy, average strength of signal, ratio of positive and average energy of X-axis signal, and ratio of positive and average energy of Y-axis signal [54]. The X- and Y-axis of the magnetic sensor are installed parallel to the earth's surface, while the Z-axis is vertically installed. [7, 43] The different types are classified into motorcycles, two-box cars, saloon cars, and sport utility vehicles in this application. Using these approaches, vehicle detection and classification applications have been developed as prototypes.

In our research, considering the cost of installation and maintenance, we use a single AMR magnetic sensor to install at the roadside. Our approach is used in an Australian road environment. The types of vehicles in Australian road traffic are typically sedans, vans, trucks and buses. In our data measurement, the X-axis is a unique factor for input data, while the Y- and Z-axes is also work as input factors. We analyse these vehicle types using measurements of how the earth's magnetic field signal changes in the time domain when a vehicle passes through our sensing area. We also explore vehicle identification and classification by extending the audio signal analysis approach. The sensor measurements of the magnetic field are processed by means of signal feature extraction and vector quantisation to achieve vehicle type classification. Our approach is presented in the following sections.

Chapter 3: Raw magnetic data measurement and collection

3.1 Raw magnetic data measurement

In Australia, vehicles travel on the left side of the road. Our experiments were conducted on a road in a Sydney suburb. The vehicle types chosen for observation on this road are sedans, vans, trucks and buses. The reason for this choice is that the raw magnetic signals of these four vehicle types exhibit significant differences. We used a single 3-axle AMR sensor to measure the earth's magnetic field changes when vehicles passed through our experimental area. The axes are the X-axis direction (right/west), Y-axis direction (in lane/south), and Z-axis direction (up). The road experiment is configured as shown in Figure 1.

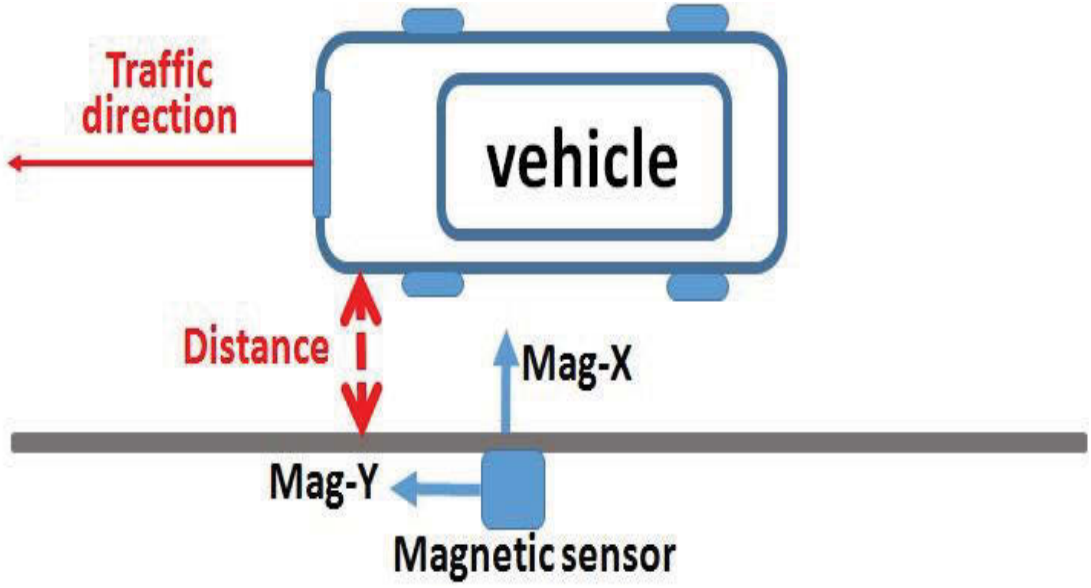

Figure 1: Road experiment configuration

The AMR sensor has three sensitive axes, namely X, Y and Z. The main X-axis provides positive main voltage change when the magnetic field increases in the sensitive axis direction [55, 56]. There is a tensor gradiometer consisting of HMC1001 and HMC1002 microcircuits, both of which are designed by Honeywell. They are one-axis and two-axis

sensors used to measure magnetic fields [43, 57]. Both are implemented vertically, so that the HMC1001 and HMC1002 microcircuits constitute an orthogonal measurement structure. These two microcircuits are simple resistive Wheatstone bridges for the measurement of magnetic fields and require a voltage of 10V [58]. This set-reset current eliminates temperature drift and nonlinear error [56]. The gradiometer structure has two segments: the main circuit board and the probe part. The main board is a voltage-stabilising module comprising a set-reset current signal module and a power supply module. The probe part consists of seven probes, each composed of one HMC1001 and one HMC1002 chip [59, 60]. Therefore, this is a three-axis framework. The main circuit board (in a box made of alloy material) and the probe part are connected by the net port to maintain signal stability [61]. We used the AMR sensor to record vehicles passing on our chosen road. The raw magnetic signals of the X-axis, Y-axis and Z-axis are shown in Figures 2, 3 and 4 respectively.

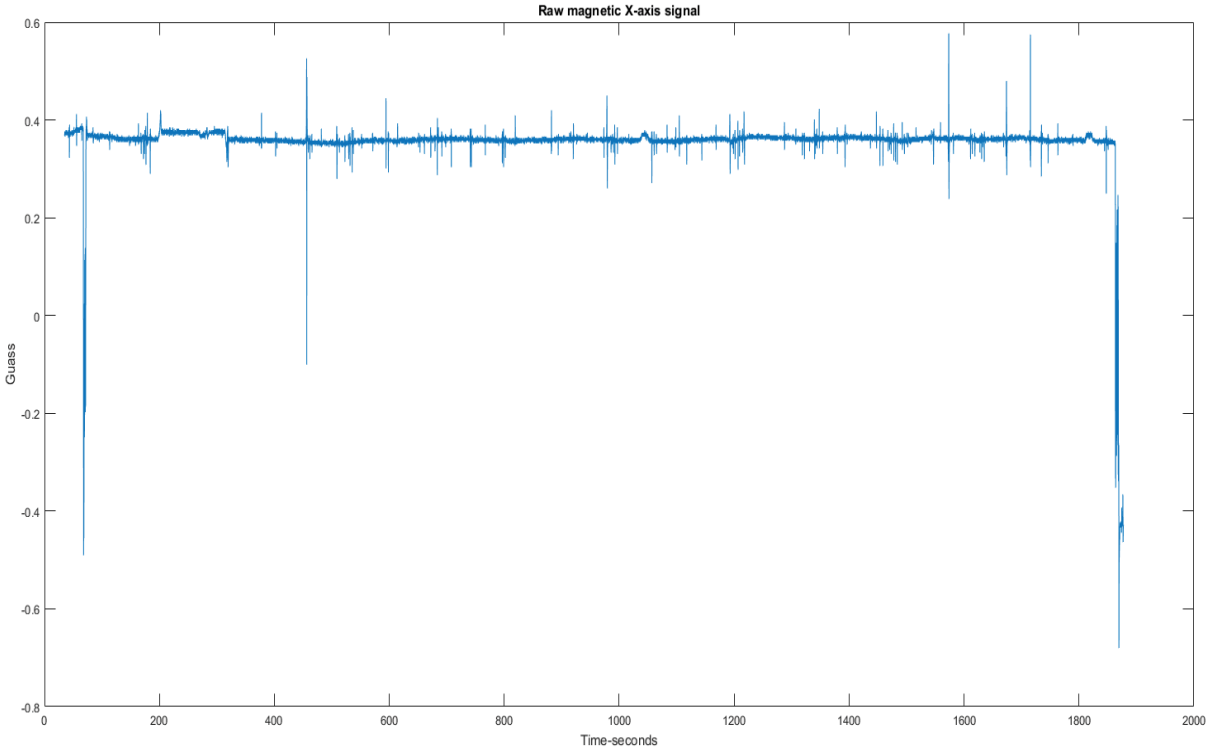

Figure 2: Road raw magnetic X-axis signal

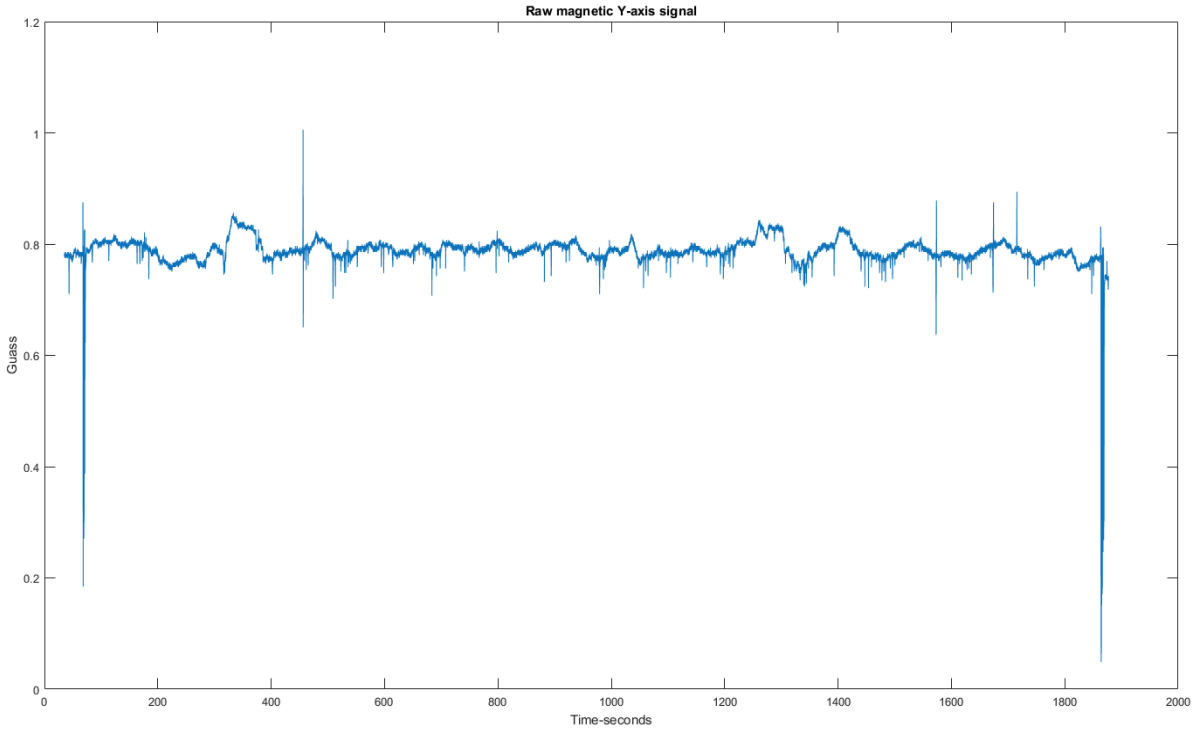

Figure 3: Road raw magnetic Y-axis signal

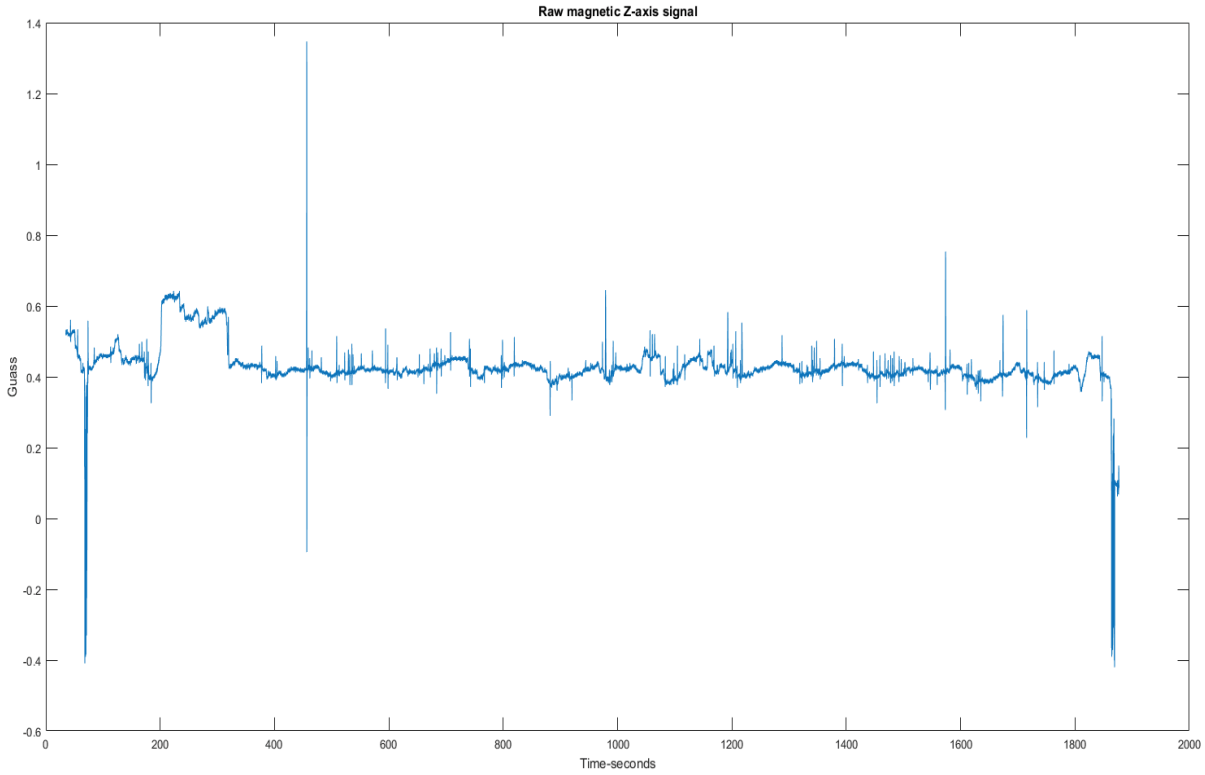

Figure 4: Road raw magnetic Z-axis signal

3.2 Raw magnetic signals in collection and category

In signal collection, the time of passing vehicles needs to be recorded in order to match the AMR sensors. There are two aspects affecting signal matching. Firstly, the position of the vehicle generates different raw magnetic signals for the same vehicle. Moreover, the data for overlapping vehicles needs to be moved so that the signal records only one vehicle passing the sensor. In this experiment, on the one hand, the sensor is fixed in the same position on the ground; on the other hand, we only record only one vehicle and set the minimal time as one second between two vehicles passing the sensor. There are two reasons. Firstly, the one second is very widely used in audio processing, because the frequent domain change rapidly. Secondly, based on the experimental results and observations, one second can achieve good performance. The ground truth of our magnetic signal is shown in Figures 5 and 6.

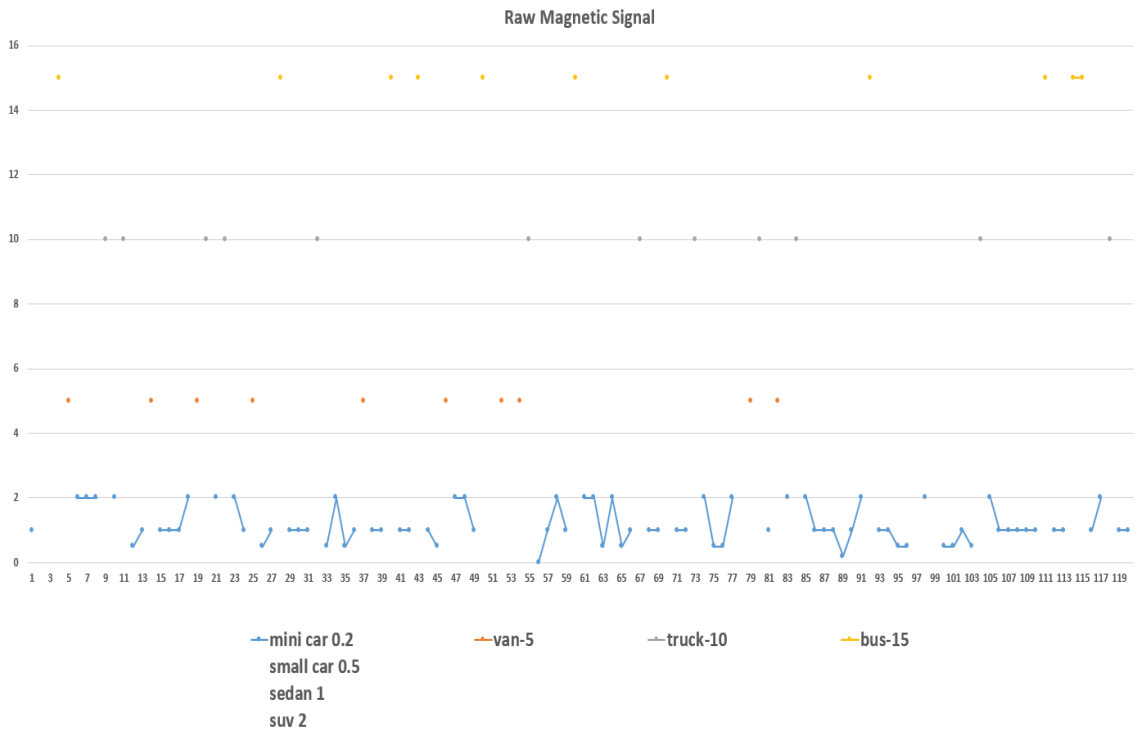

Figure 5: Road raw magnetic vehicle passing record signal_1

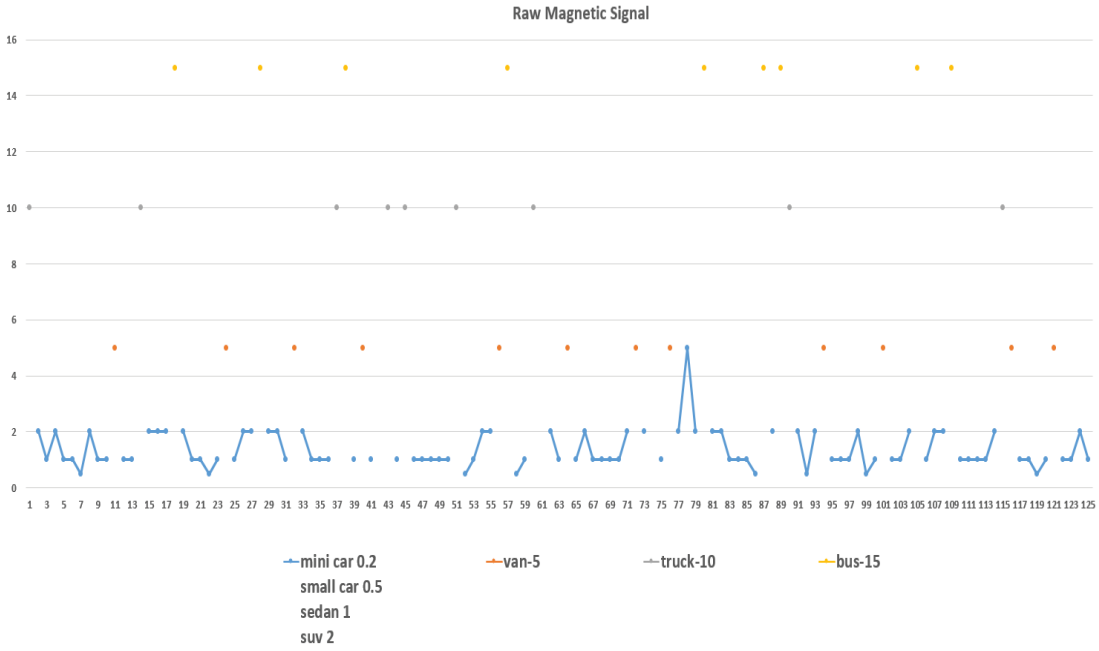

Figure 6: Road raw magnetic vehicle passing record signal_2

Chapter 4: Classification within one-dimensional map in magnetic field

4.1 One-dimensional map framework overview

This model is based on the Mel-Frequency Cepstral Coefficients (MFCC) and Vector Quantisation (VQ). Further details are presented in Figures 11, 12 and 13. In our research, we analyse MFCC for audio systems and VQ to analyse the magnetic field measurement data for passing vehicles. The audio features of MFCC represent the characteristics of the human sound system [62, 63]. Vector Quantisation is a lossy data compression method for audio signals [64]. VQ can transform several scalar data into one vector data and quantise a whole vector space [65, 66]. For the identification and classification of vehicle signals, we first extract the features, then classify them into different types of vehicles. The process is outlined below.

Looking at the feature extraction process in the literature, MFCC has been used to extract speech signal features in speech recognition systems [64]. Audio signal features include speech speed, speech fragment length, speech frequency, and amplitude [62]. In road vehicle recognition, when a vehicle passes through the sensing area, the magnetic field in that area will change and accordingly cause magnetic measurement changes. These changes are displayed as a signal wave in measurement. From the observation of vehicle types on the road, we classify and analyse road vehicles into four types: sedan, van, truck, and bus. When these vehicles pass through the experimental zone, the magnetic sensor displays signal changes in the form of waves. The signals in the figures below provide examples of sensor measurements for these types of vehicles.

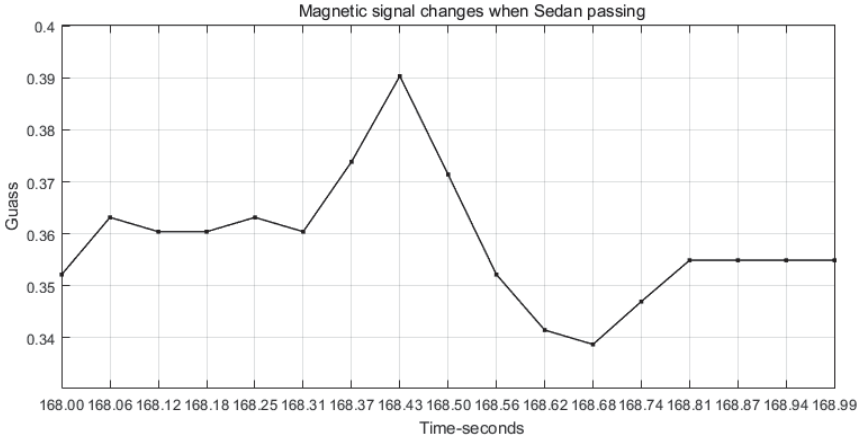

Figure 7: Magnetic sensor measurement of sedan signal

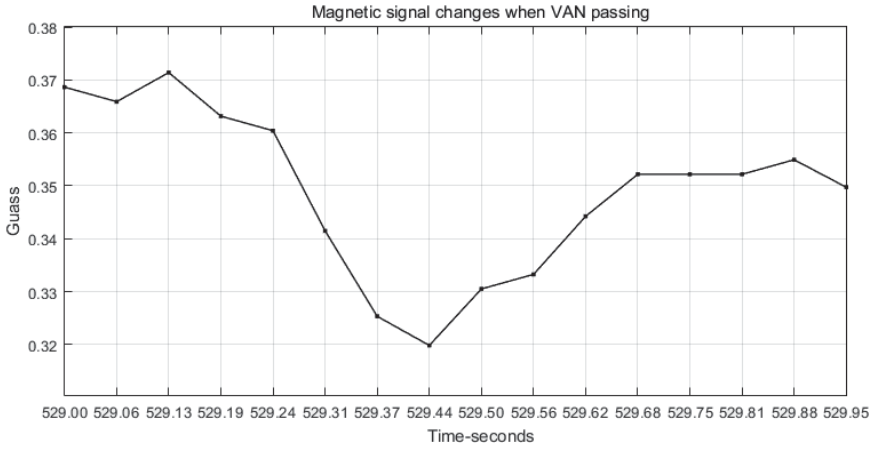

Figure 8: Magnetic sensor measurement of van signal

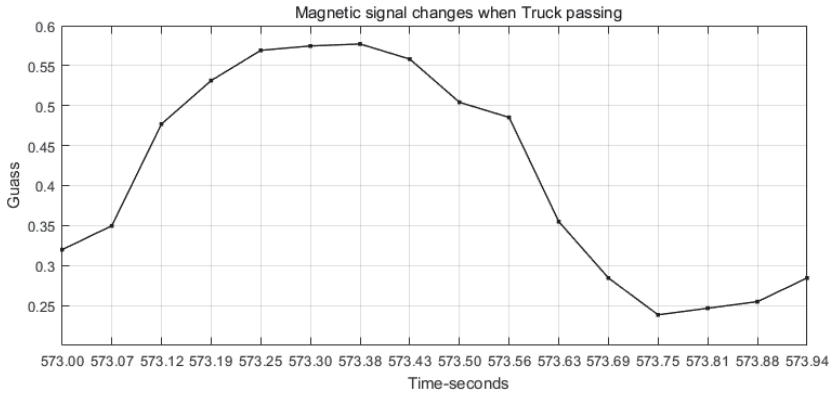

Figure 9: Magnetic sensor measurement of truck signal

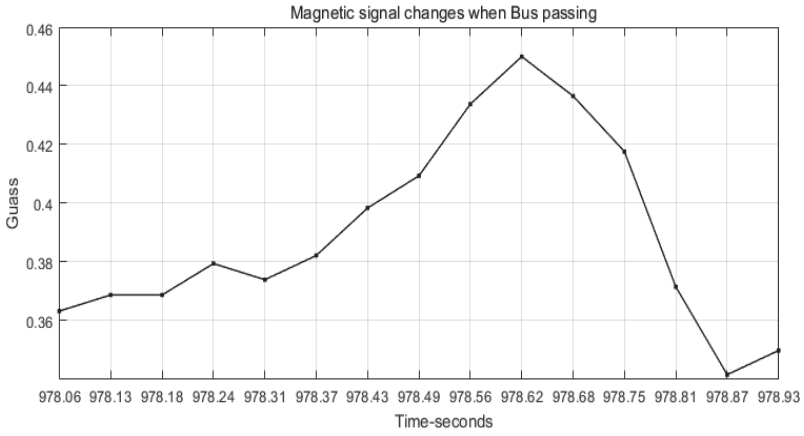

Figure 10: Magnetic sensor measurement of bus signal

4.2 Vehicle feature extraction in one-dimensional map

From the experiments, we found that magnetic signal waves and audio waves display similar characteristics, such as reflection, refraction, intervene, and diffraction. In the time and frequency domains, the speed, length, and frequency of signal waves have a certain relationship for both magnetic waves and audio waves [67]. In our research, we explore the signal feature extraction to analyse magnetic field signal features. The process flow of the magnetic field feature extraction is presented in Figure 11.

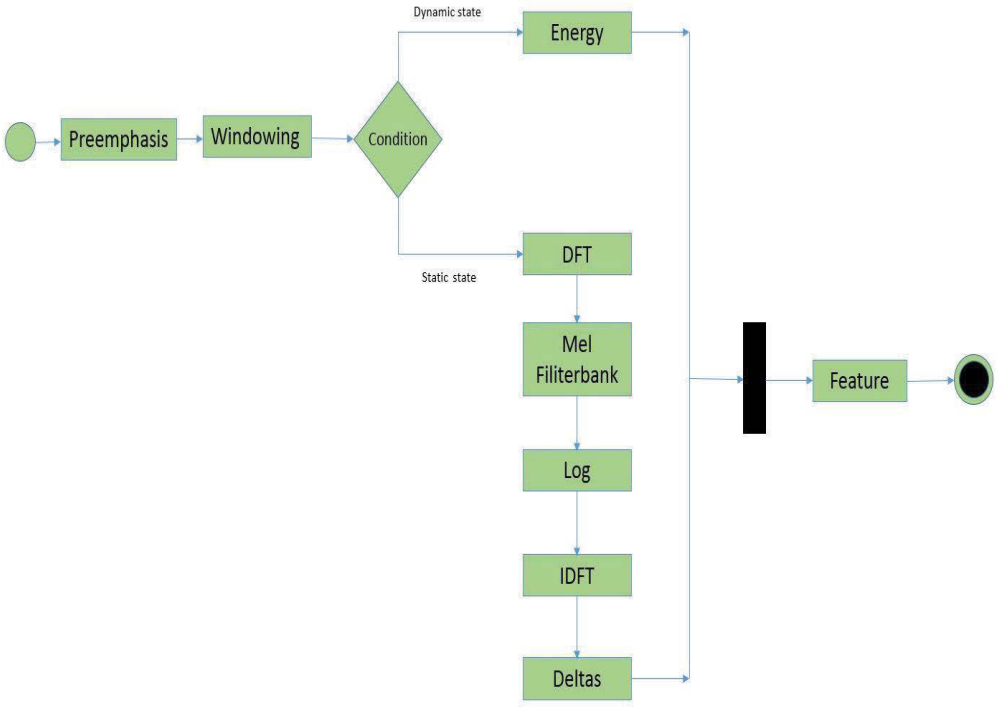

Figure 11: Magnetic measurement feature extraction

Pre-emphasis

The first step of magnetic signal feature extraction is "pre-emphasis". This step improves the energy in high frequencies and balances the energy from lower and higher frequencies. In the time domain, the filter equation is as below:

$$y[n] = x[n] - \alpha x[n-1]. \quad (1)$$

where *n* is the time, x[n] is the input signal, and $0.9 \leq \alpha \leq 1$.

Windowing

In the second step, "Windowing", we extract signal features from a small signal window. The windowing process is performed using the signal value and window value. If the value of the signal at time *n* is $s[n]$, and the value of the window at time *n* is $w[n]$, the signal value y[n] of this windowing process can be expressed using the following equation:

$$y[n] = w[n]s[n]. \quad (2)$$

In order to shrink the values of the signal toward zero at the window boundaries and avoid discontinuities, we further define two windowing functions: "Rectangular" and "Hamming".

"**Rectangular**":

We set the window to 1 when signal time *n* is between 0 and *L*-1, where *L* is the length of the frame of the signal. In other time periods, we set the window to 0.

$$w[[n] = \begin{cases} 1 & 0 \leq n \leq L-1 \\ 0 & otherwise \end{cases}. \quad (3)$$

"**Hamming**":

The goal of the Hamming window is to extract the spectral features, not from the entire signal, but from a small signal window [28].

$$w[n] = \begin{cases} 0.54 - 0.46\cos\frac{2\pi n}{L} & 0 \leq n \leq L-1 \\ 0 & otherwise \end{cases}. \quad (4)$$

After the "Windowing" process is complete, the distributed frames will result in two states: a dynamic state and a static state. The feature extraction process will go through

two different flows, as seen in Figure 6. After "Windowing" processing, there is a condition that processes each frame for its magnetic features. There are two steps, including the dynamic and static states, due to the reason of each frame undergoing "Windowing".

The windowing process includes "frame shift" and "frame size". It is difficult to extract an entire feature from the magnetic feature as the spectrum changes very fast. Therefore, in the frame state, two conditions are imposed to resolve this issue: *dynamic state* and *static state*. The *dynamic* processing is caused by a frame *shift* of 10ms, while the *static* state refers to frame *size*, which is 25ms. Therefore, the total feature is the data of both dynamic and static states.

Discrete Fourier Transform (DFT)

For the static frame condition, the third step is a Discrete Fourier Transform (DFT). We extract magnetic information for the windowed signal and calculate how much energy the signal contains at different frequency bands.

The DFT is defined as follows:

$$x[k] = \sum_{n=0}^{N-1} x[n] e^{-j2\frac{\pi}{N}kn}, \quad (5)$$

where *k* and *N* are the sequence of frame and discrete frequency bands respectively, and e, θ are presented in Euler's formula:

$$e^{j\theta} = \cos\theta + j\sin\theta. \quad (6)$$

Mel Filter Bank

The next steps of feature extraction are "Mel Filter Bank" and "Log Processing" for reduction to lower amplitudes. This is computed using:

$$mel(f) = 1127In^{(1+\frac{f}{700})}, \quad (7)$$

where *f* is the frequency of the input signal.

The final steps are "Inverse Discrete Fourier Transform" (IDFT) and "Deltas" and "Energy": therefore, the magnetic feature includes Cepstrum, Deltas and Energy.

Inverse Discrete Fourier Transform (IDFT)

IDFT is computed using the following equation:

$$c[n] = \sum_{n=0}^{N-1} log^{(|\sum_{n=0}^{N-1} x[n]e^{-j\frac{2\pi}{N}kn}|)} e^{j\frac{2\pi}{N}kn}, \quad (8)$$

where c is the cepstrum of the magnetic feature, and the inverse DFT of the log magnitude of the DFT of a signal.

Delta

In the Delta stage, we compute the gap cepstrum. Gap cepstrum is defined as the value of the average of the current cepstrum and the cepstrum of the next time. Gap cepstrum d is computed as follows:

$$d(t) = \frac{c(t+1)-c(t-1)}{2}. \quad (9)$$

Dynamic state

For the dynamic state frames after "Windowing", we start the "Energy" process as in Figure 6.

Energy

Energy is computed using the energy of the frame between two time points t1 and t2:

$$Energy = \sum_{t=t_1}^{t_2} x^2[t]. \quad (10)$$

Feature

For both process flows for dynamic state and static state (see Figure 11), the final features are integrated.

The magnetic feature is presented using an integration of cepstrum c, Energy, and the gap cepstrum d (as in Equations 8, 9, and 10).

Vehicle magnetic features are consequently extracted and represented via this process.

4.3 Vehicle classification in one-dimensional map

To classify magnetic sensor signals for vehicle types, we transform several scalar magnetic measurement data into one vector [43]. We design this vector as containing cepstrum *c*, *Energy*, and the gap cepstrum *d*, which are extracted via the vehicle magnetic feature extraction process. A vector space is then quantised using all magnetic feature vectors. We compress the data and store this feature information in magnetic vector space [68, 69]. We design this classification process as shown in Figure 12.

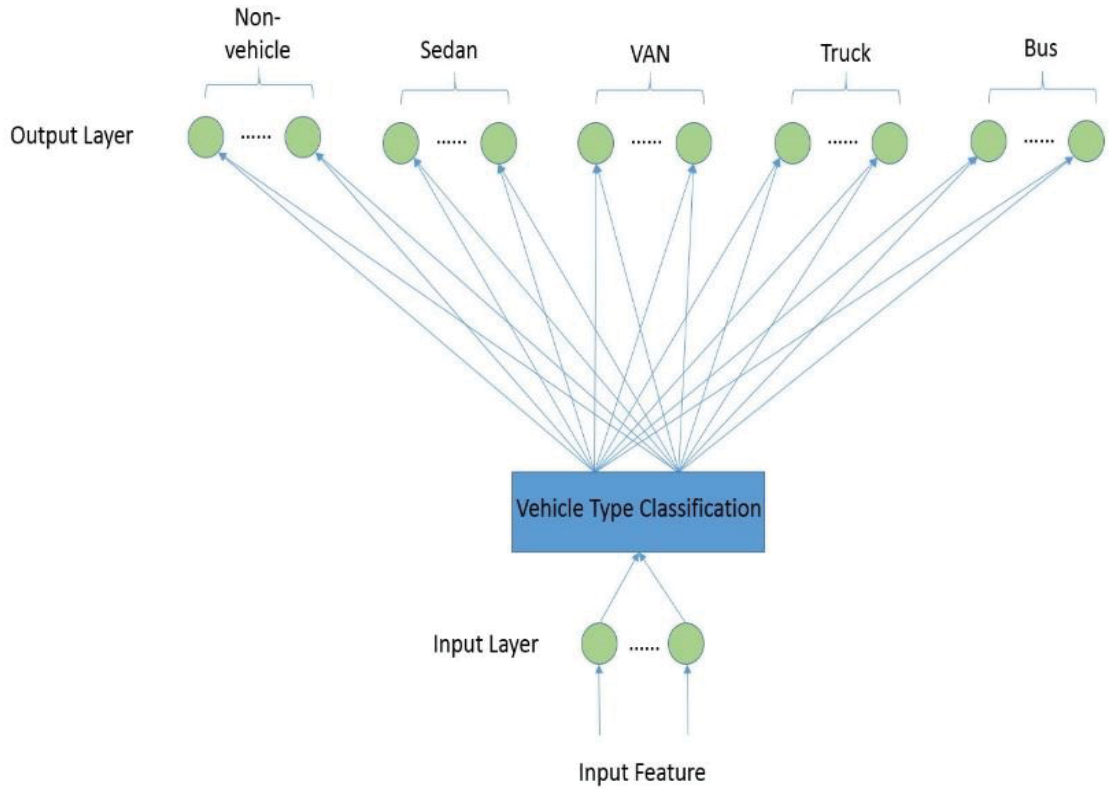

Figure 12: Vehicle magnetic feature vector quantisation classification process

When there is no vehicle in the measurement area, the magnetic sensor output signals are the earth's magnetic field and environmental noises. In this process, we also define a "Non-vehicle" type when vehicles are absent. Accordingly, in our experiments, the signal

types are: sedan, van, truck, bus and non-vehicle. We design a one-dimensional classification map to present the distribution of vehicle types, as shown in Figure 13.

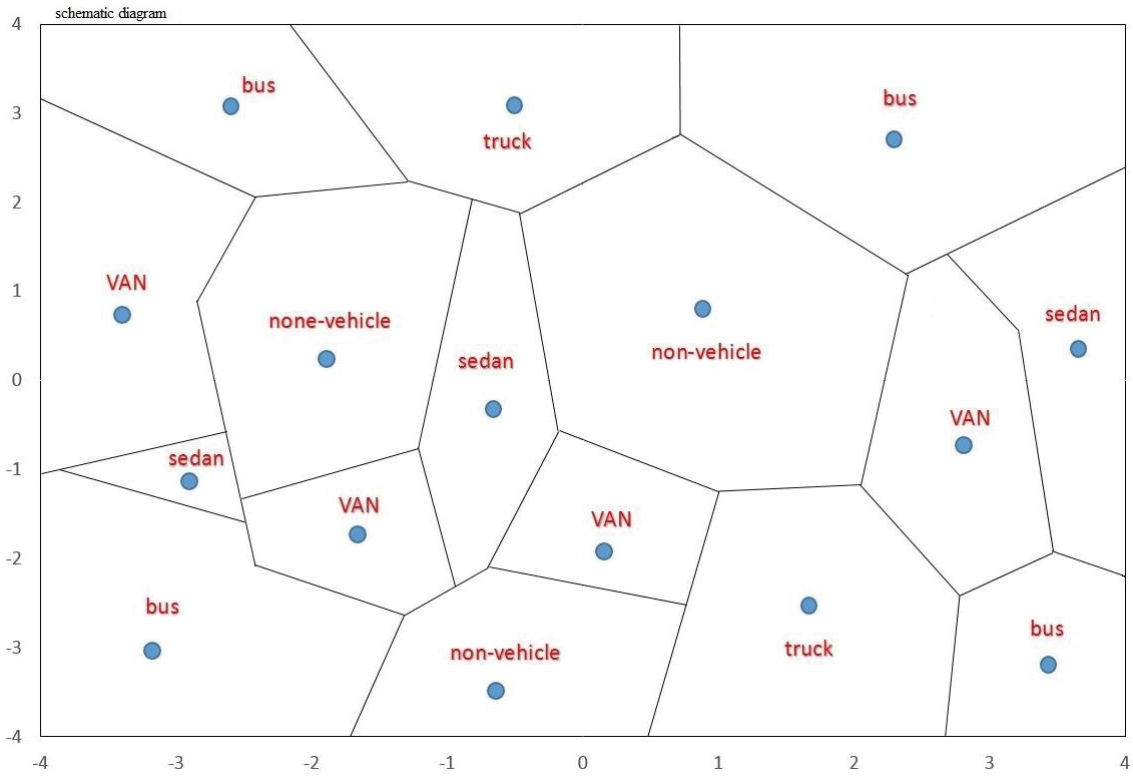

Figure 13: Distribution of vehicles on one-dimensional classification algorithm

In this distribution map, we designate a pair of numbers as the coordinate. Every point based on x-axis value (X- axis direction) is the earth's magnetic value. The one-dimensional map has two axes, both of which are x-axis values. Every point has its own unique position. The coordinate is displayed in one region at an approximated position by a blue circle in that region. We uniquely represent each region using this coordinate. For example, we designate the coordinate [-0.5, 0] to represent the position of one passing sedan in this distribution [70, 71].

There are 16 regions and 16 blue circles in total, as shown in Figure 13.

In the classification algorithm, we label the vector data for feature classification training as $T = \{x_1, x_2, \dots, x_m\}$. We use 2/3 of the entire magnetic feature data as training data. We then divide the magnetic feature vector space (classification) into N (5) parts. Let $C = \{c_1, c_2, \dots, c_N\}$ represent a codebook, where c is the codevector. This codebook contains all magnetic feature vectors. S_n is the encoding region with codevector c_n . We then set

the entire vector space $P = \{S_1, S_2, \dots, S_N\}$. If X_m is in the S_n area, it can therefore be approximately regarded as c_n: $Q(x_m) = c_n$. We define the distortion of the magnetic vector that obtains the original vector, instead of the changed vector, in order to acquire accurate output data.

The average distortion D_{ave} can be computed as follows:

$$D_{ave} = \frac{1}{Mk}\sum_{m=1}^{M}|x_m - Q(x_m)|^2. \quad (11)$$

We design optimality criteria using the "Nearest Neighbour Condition" and "Centroid Condition".

These criteria are expressed as follows:

"**Nearest Neighbour Condition**":

$$S_n = \{x: |x - c_n|^2 \leq |x - c_{n'}|^2 \ \forall n' = 1,2, \dots, N\}. \quad (12)$$

The vectors standing on the boundary can be chosen to a certain region *Sn.*

"**Centroid Condition**":

$$c_n = \frac{\sum x_m \in s_n^{X_m}}{\sum x_m \in s_n^1} \ n = 1,2, \dots, N. \quad (13)$$

If the transformed vehicle magnetic vector meets both the "Nearest Neighbour Condition" and "Centroid Condition", then the magnetic vector can be classified into that vehicle type.

Chapter 5: Classification within three-dimensional map in magnetic field

5.1 Three-dimensional map framework overview

In the one-dimensional map section above, we present a road vehicle identification and classification approach using magnetic sensor and magnetic signal feature extraction and classification. In order to reduce the deployment, interruption of road traffic and maintenance costs, we use a roadside magnetic sensor to detect the vehicles. The magnetic signal processing approach extends MFCC to extract the magnetic signal features and classify them into four types of vehicle signals: sedan, van, truck and bus. When vehicles pass by the experimental spot, the magnetic field measurements display signal changes in the form of waves. Figure 14 illustrates the magnetic field changes in one dimension for these types of vehicles.

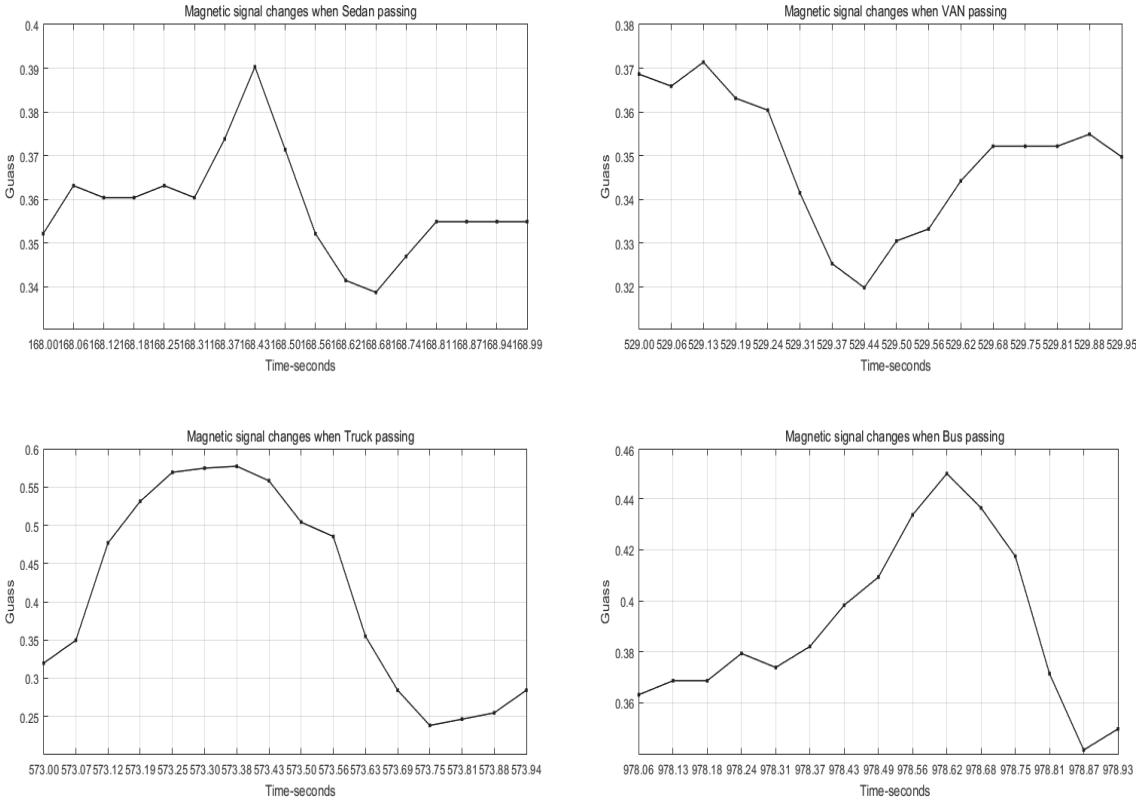

Figure 14: Magnetometer measurements of four types of vehicles

Accordingly, in our experiments, the five signal types are: sedan, van, truck, bus and non-vehicle. When there is no vehicle in the measurement area, the magnetic sensor output signals are the earth's magnetic field and environmental noises.

We design this classification process as in Figure 15.

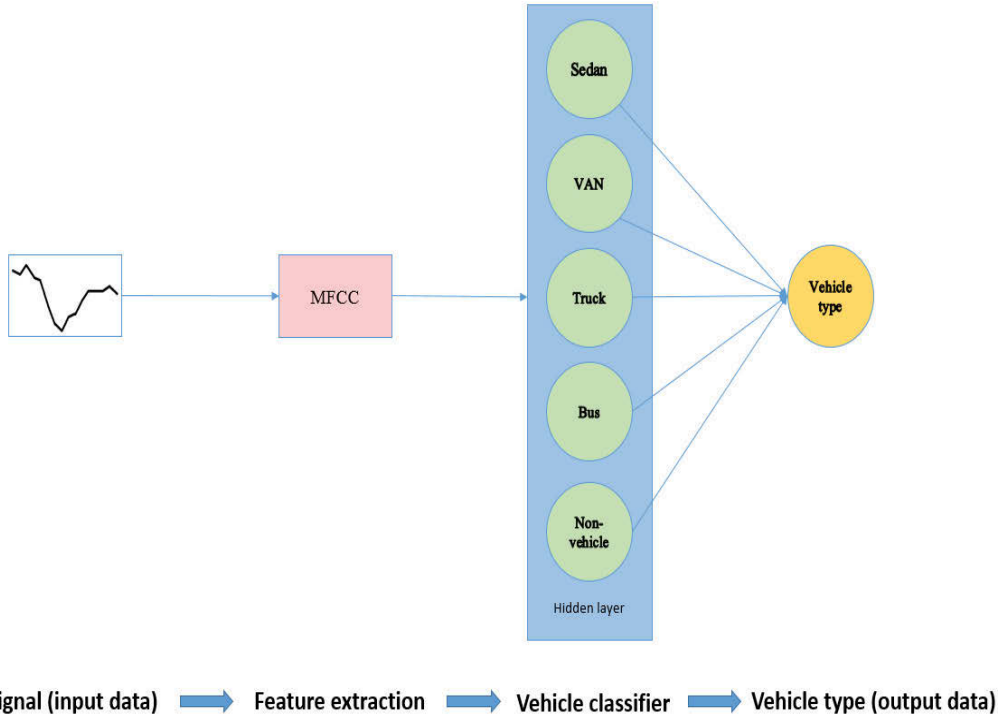

Figure 15: Vehicle magnetic feature extraction and classification process

In our research, we use Dynamic Time Warping (DTW) to filter the raw measurement signal and analyse Mel-Frequency Cepstral Coefficents (MFCC) for audio systems and Vector Quantisation (VQ) to classify magnetic field measurement data for passing vehicles. Unlike the one-dimensional map, this three-dimensional map also focuses on the other two axis values: the y-axis and z-axis.

In the identification and classification of vehicle signals, we filter the raw magnetic field measurement signals, extract the relative features, and then assign these features to different types of vehicles. The method is presented below.

5.2 Dynamic time warping selection process

Dynamic time warping (DTW) is a process used to compare signals and align sequences between two time series. Under some boundary and temporal consistency constraints, DTW is a point-to-point method that can obtain a global optimal solution via cost matrix [72, 73].

The two 'van' magnetic signals are compared and selected using DTW, as illustrated in Figure 16. Figure 16 displays that there are 16 points. Each point has been compared between two magnetic signals. The original magnetic signal compared with another magnetic signal, after which the signal output is aligned. Here, the Euclidean distance is 0.131226. In our experiment, there are 53 sedans, 22 vans, 21 trucks, 20 buses and 92 non-vehicle types of raw measurement signals. We compare each magnetic signal using DTW and the resulting values are different. In the end, there are 52 sedans value, 21 vans value, 20 trucks value, 19 buses value and 91 non-vehicle value of signals processed by DTW. According to the different value results, the similar value can be selected as training dataset.

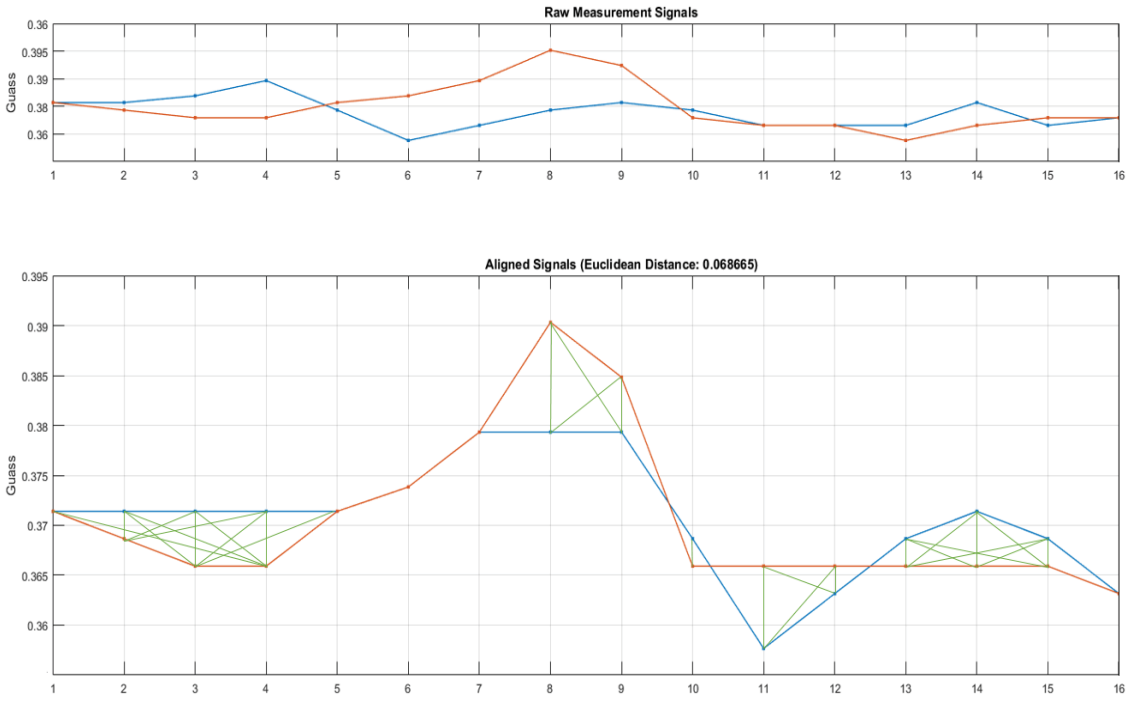

Figure 16: Two 'van' magnetic signals compared and selected using DTW

Figures 17, 18, 19 and 20 below identify each raw magnetic 'van' measurement signal compared with other 'van' signals. The value is the distance between two van signals. For

example, in Figure 17, each raw magnetic van measurement signal is compared with VAN_2, such that there are 19 values processed by the DTW algorithm. In this process, we use all 'van' raw magnetic measurement signal to compare with each other and select the 19 nearest values. Consequently, 20 raw magnetic 'van' measurement signals can be selected for our following experiment. Similarly, the same methods were used for the bus, truck and sedan types to select 19, 20 and 52 values. Therefore, there are 20 'bus', 21 'truck' and 53 'sedan' raw magnetic measurement signals in the following experiment.

In Figure 17, the result is 21 values and 22 vans selected.

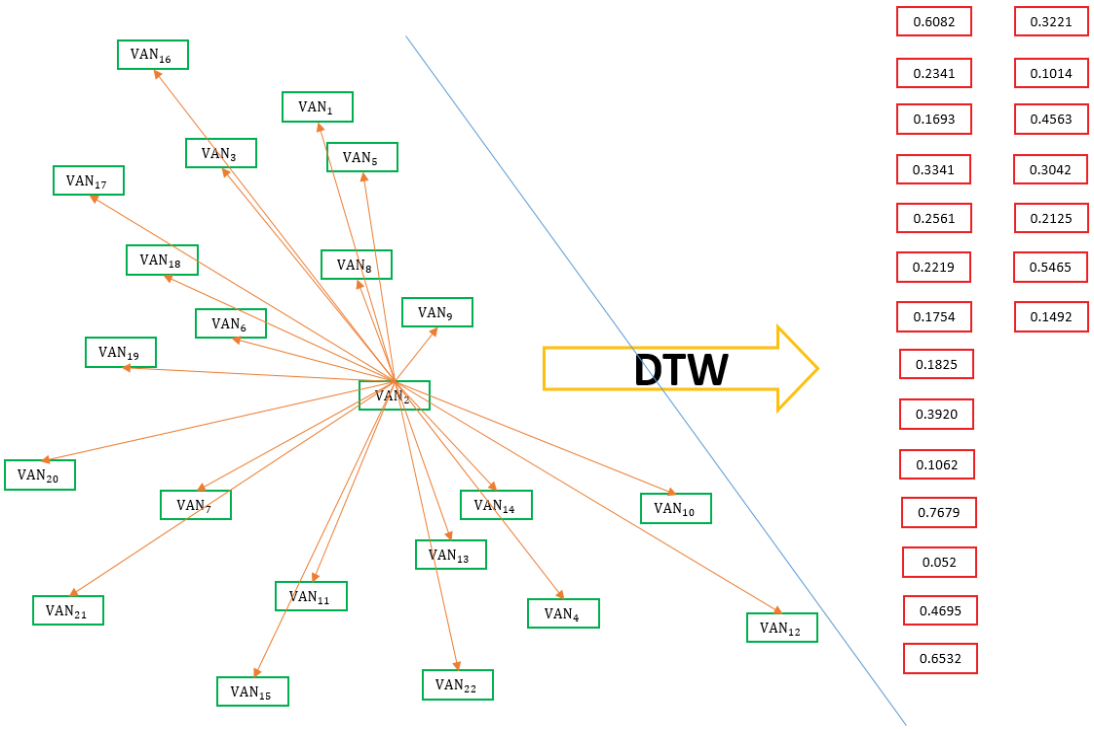

Figure 17: The value of Van magnetic signals compared using DTW

In Figure 18, the result shows 19 values and 20 buses selected.

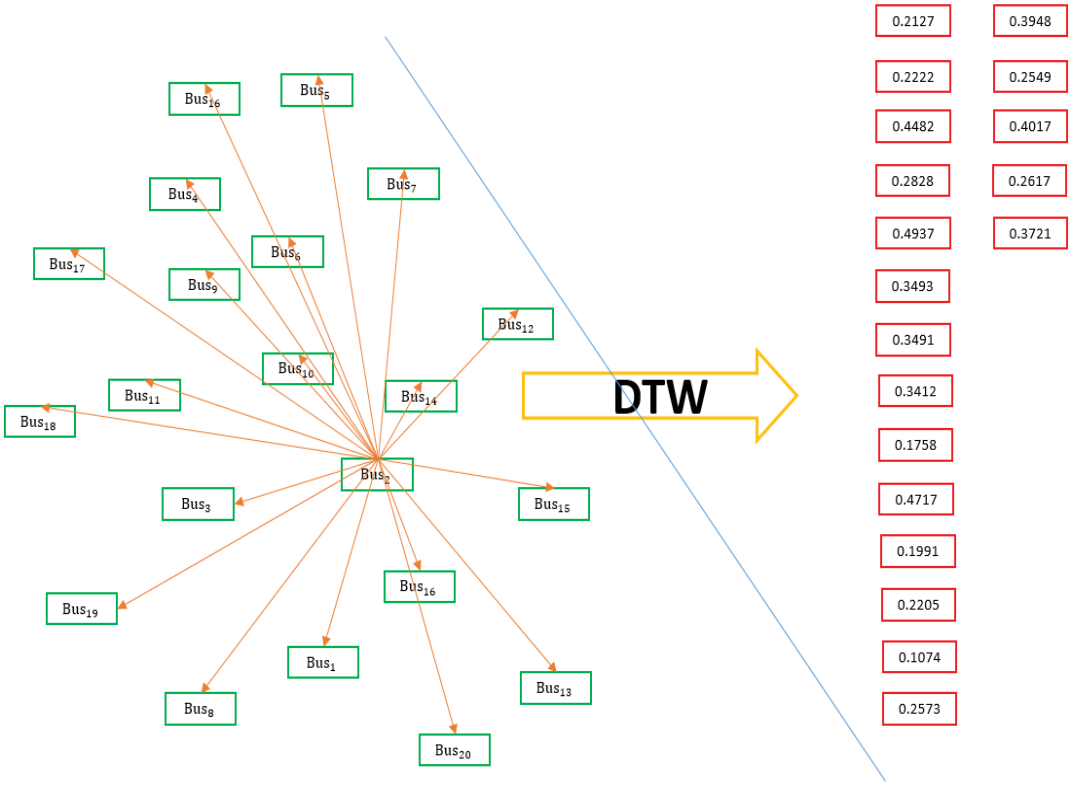

Figure 18: The value of Bus magnetic signals compared using DTW

The result of Figure 19 displays 20 values and 21 trucks selected.

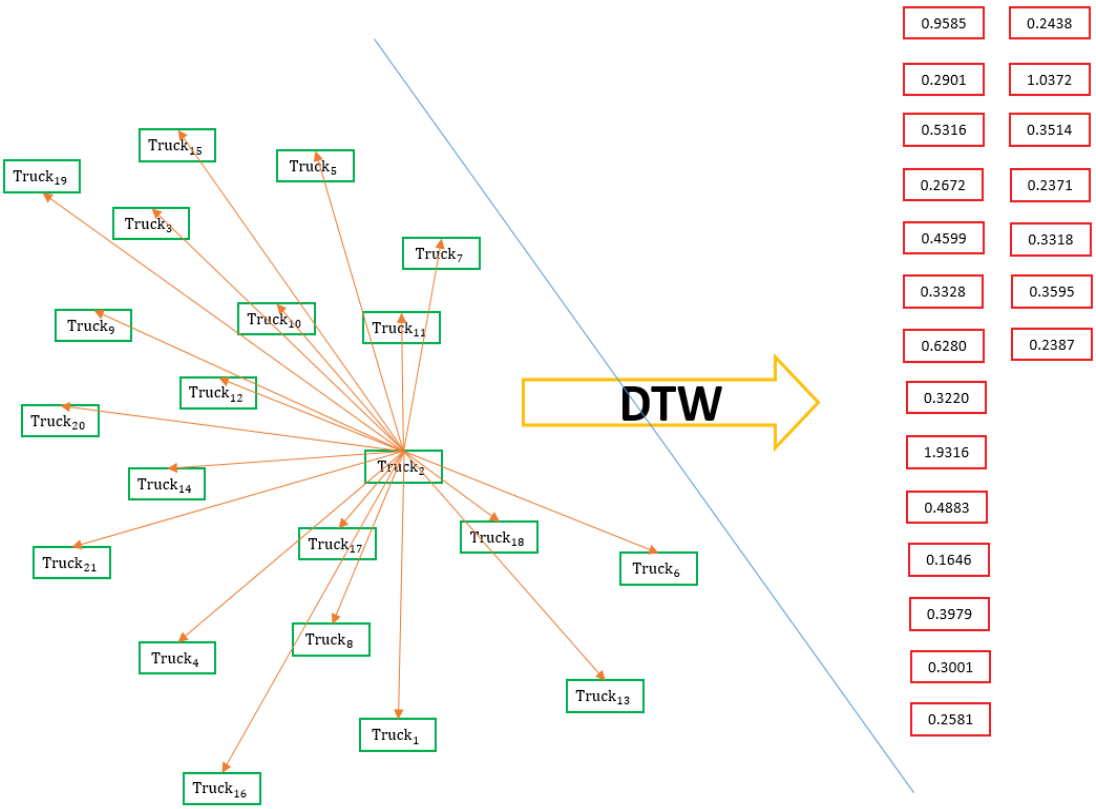

Figure 19: The value of Truck magnetic signals compared using DTW

In the last DTW process, the result of Figure 20 shows there are 52 values and 53 sedans selected.

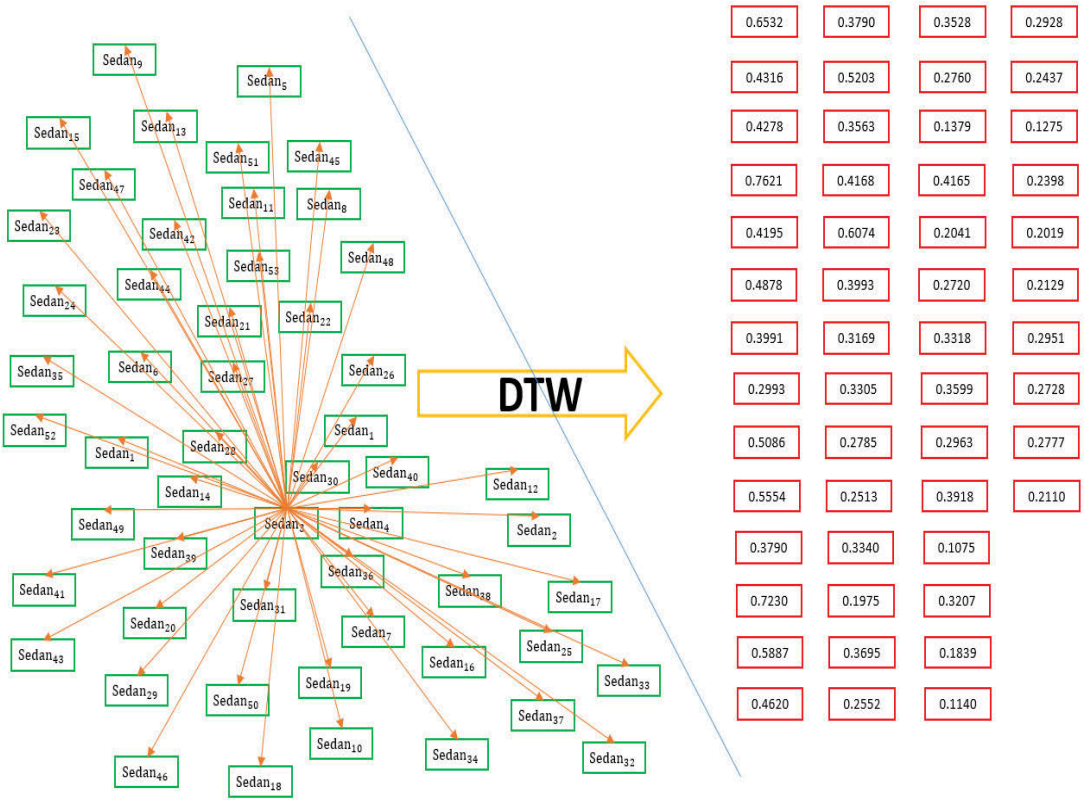

Figure 20: The value of Sedan magnetic signals compared using DTW

5.3 Vehicle feature extraction in three-dimensional map

The process flow of magnetic field feature extraction is the same as in Figure 11. Each step of the process has been presented in the earlier section.

Vehicle magnetic features are consequently extracted and represented according to this process.

5.4 Vehicle classification in three-dimensional map process

We design a three-dimensional classification model to present the distribution of vehicle types (see Figure 21). As for the one-dimensional classification model, VQ is still used as a classifier in this method.

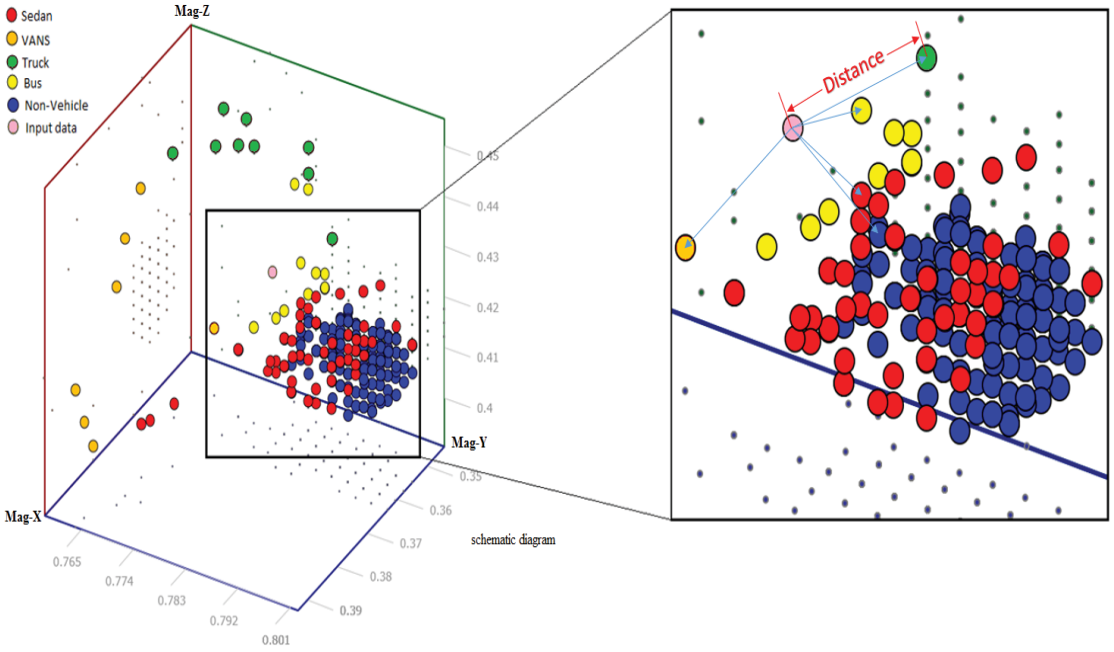

Figure 21: Distribution of vehicles on three-dimensional classification algorithm

As shown in Fig. 21, the three dimensions indicate the three directions of the magnetic field: i.e., X-axis direction (right/west), Y-axis direction (in lane/south), and Z-axis direction (up). The sample points indicated by coloured circles in Fig. 21 represent different vehicles. We uniquely represent each colour circle using this coordinate. We define $s = \{p_1, p_2, \dots, p_n\}$ and use s to indicate every sample point $(p_1, p_2, \dots, p_n)$ in Fig. 21, while x, y and z are used to represent the coordinates in the X, Y and Z-axis direction. Represent x, y and z as the earth's magnetic value respectively, which is computed using the below:

$$P = \sqrt[2]{x^2 + y^2 + z^2}. \tag{14}$$

In this case, we designate sedans as red circles, vans as orange circles, trucks as dark red circles, buses as yellow circles, non-vehicles as blue circles, and input data as pink circles (Figure 21). For example, the coordinate [0.352, 0.412, 0.786] represents the position of one passing sedan in this distribution. The VQ algorithm compares the distance between input data (pink circle) and other vehicles (red/orange/green/yellow/blue circles). For example, if the distance between the input data (pink circle) and Bus (yellow) is the shortest, the output data is 'Bus'. Similarly, each input data point has a corresponding vehicle in this three-dimensional space.

Chapter 6: Experimental results

6.1 Results for magnetic field in one-dimensional map

In this section, we perform classification experiments for our vehicle types (sedan, van, truck, bus and non-vehicle) based on signal features obtained from the magnetic feature extraction algorithm. In the vehicle type classification modelling process, we separate the magnetic measurement data into two sets: training data and testing data. We analyse the vehicle type classification using two groups of experiments with six different data configurations. In Experiment Group 1, we use a data set of 36 sedans, 8 vans, 7 trucks, 10 buses and 87 non-vehicle signals. In Experiment Group 2, we use 73 sedans, 15 vans, 14 trucks, 15 buses and 174 non-vehicle signals. Moreover, for each group, we set up training and testing data using three types of data configuration. This makes six types of experiments in total, as shown in Table 1.

Table 1: Data configuration for two groups of experiments using the one-dimensional map

Group 1			**Group 2**		
36 sedans, 8 vans, 7 trucks, 10 buses and 87 non-vehicle signals			73 sedans, 15 vans, 14 trucks, 15 buses and 174 non-vehicle signals		
Data configuration			**Data configuration**		
	Training data	Testing data		Training data	Testing data
Experiment 1	2/3	1/3	Experiment 4	2/3	1/3
Experiment 2	3/4	1/4	Experiment 5	3/4	1/4
Experiment 3	4/5	1/5	Experiment 6	4/5	1/5

Magnetic dataset is an approach for the accuracy of the feature extraction process and classification in test. In our report, we divide it into 2 groups and 6 experiments. Firstly, we divide the entire data pool into training and testing sets comprising 2/3 and 1/3 of the data respectively. All training and testing data are selected at random. After that, we change the rate of training and testing sets at random to identify the accuracy that is not

relative to pick up date. The testing and training rate change to 1/4 and 3/4 respectively. The accuracy for each type of vehicle increases, as shown in the below table, in experiments 1 and 2. Subsequently, the rates change from 1/4 and 3/4 to 1/5 and 4/5 respectively. The accuracy results also increase, as noted. This is due to the increase in the random training set for perfecting the training vector quantisation. If we continue to increase the training rate to determine whether the training rate will influence the testing accuracy, the rate will stabilise at a maximum. We can see these results in experiments 1 and 2. In experiment 1, we deploy a date number of 148, while in experiment 2, we provide a double date of 291. The magnetic dataset is presented in figure 22.

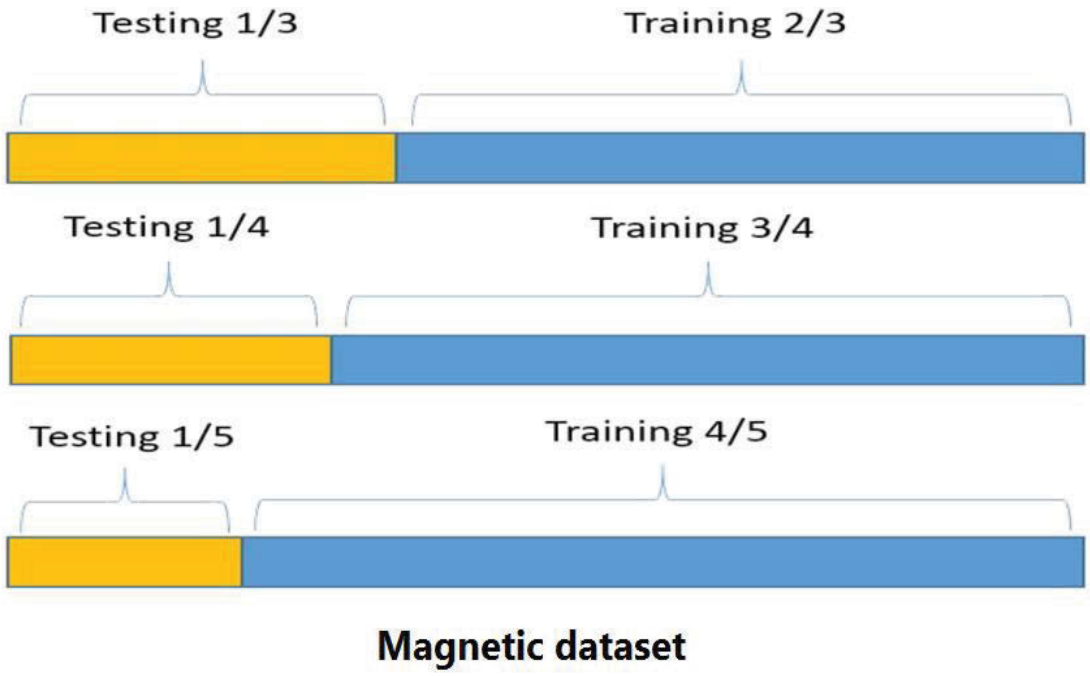

Figure 22: Magnetic dataset in the two experiments

In Experiment 1, we use 2/3 of the entire measurement data as input for the algorithm, and 1/3 as result testing data. The classification results are presented in Table 2. This table shows the observed vehicle type, training data number, testing data number, successful classified vehicle number, and algorithm accuracy in Experiment 1.

Table 2: Experiment 1 results: Vehicle classification using 2/3 of measurement data as training data and 1/3 data as testing data for one-dimensional map

	Sedan	Van	Truck	Bus	Non-vehicle
Observed	36	8	7	10	87
Training data	24	5	4	6	58
Testing data	12	3	3	4	29
Algorithm classification	7	1	1	1	18
Algorithm accuracy	58%	33%	33%	25%	72%

The results of Experiment 2 are presented in Table 3.

Table 3: Experiment 2 results: Vehicle classification using 3/4 of measurement data as training data and 1/4 of measurement data as testing data for one-dimensional map

	Sedan	Van	Truck	Bus	Non-vehicle
Observed	36	8	7	10	87
Training data	27	6	5	7	66
Testing data	9	2	2	3	21
Algorithm classification	7	1	1	1	18
Algorithm accuracy	78%	50%	50%	33%	86%

In Experiment 3, we alter the training data set such that it contains 4/5 of measurement data, while 1/5 of the data becomes testing data. The results are presented in Table 4.

Table 4: Experiment 3 results: Vehicle classification using 4/5 of measurement data as training data and 1/5 of measurement data as testing data for one-dimensional map

	Sedan	VAN	Truck	Bus	Non-vehicle
Observed	36	8	7	10	87
Training data	32	6	6	8	70
Testing data	4	2	1	2	17
Algorithm classification	3	1	1	1	14
Algorithm accuracy	75%	50%	100%	50%	82%

From the results of Experiment Group 1 (see Tables 2, 3 and 4), we find that the algorithm accuracy level increases when we increase the training ratio. However, if we set the ratio of training data to testing data very high, the accuracy level will eventually stabilise. The classification results of Group 2 are as in Tables 5, 6, and 7. In Experiment 4, as shown in Table 5, we use 2/3 of the entire data as training data to classify vehicle types, while the remaining 1/3 is used as testing data.

Table 5: Experiment 4 results: Vehicle classification using 2/3 of measurement data as training data and 1/3 of measurement data as testing data for one-dimensional map

	Sedan	Van	Truck	Bus	Non-vehicle
Observed	73	15	14	15	174
Training data	48	10	9	10	116
Testing data	25	5	5	5	58
Algorithm classification	20	2	2	2	53
Algorithm accuracy	80%	40%	40%	40%	91%

Table 6 shows the results of Experiment 5 for Group 2. We increase the training data input to 3/4 of the entire set of measurement data to classify the types, while 1/4 of the data is used as testing data.

Table 6: Experiment 5 results: Vehicle classification using 3/4 of measurement data as training data and 1/4 of measurement data as testing data for one-dimensional map

	Sedan	Van	Truck	Bus	Non-vehicle
Observed	73	15	14	15	174
Training data	55	11	10	11	130
Testing data	18	4	4	4	44
Algorithm classification	15	2	2	2	40
Algorithm accuracy	83%	50%	50%	50%	91%

In Experiment 6, we further increase the proportion of training data: 4/5 of measurement data is used as training data to classify the vehicle types, while the remaining 1/5 becomes testing data. The results are shown in Table 7.

Table 7: Experiment 6 results: Vehicle classification using 4/5 of measurement data as training data and 1/5 of measurement data as testing data for one-dimensional map

	Sedan	VAN	Truck	Bus	Non-vehicle
Observed	73	15	14	15	174
Training data	60	12	11	12	140
Testing data	13	3	3	3	34
Algorithm classification	11	2	2	2	31
Algorithm accuracy	85%	67%	67%	67%	91%

From the above three tables for Group 2, we can draw two distinct findings.

Finding 1: The algorithm accuracy level is increased when we increase the total proportion of training data relative to testing data.

Finding 2: When we continually increase the ratio of training data to testing data, the accuracy level eventually stabilises.

6.2 Results for Magnetic field in three-dimensional map

We also carried out experiments on vehicle classification using three-dimensional map, which is more challenging than using one-dimensional map. With three-dimensional data, we randomly selected 1/4 of the raw data as testing data. The rest of the data is used for training. To ensure the training data can represent the characteristics of the whole dataset, DTW has been applied for training data selection. Four categories, i.e. sedan, van, truck, and bus, are classified. In Experiment, the data set contains 53 sedans, 22 vans, 21 trucks, 20 buses and 92 non-vehicle signals. We applied four-fold cross validation to make the classification results reliable. The cross-validation is presented in figure 23.

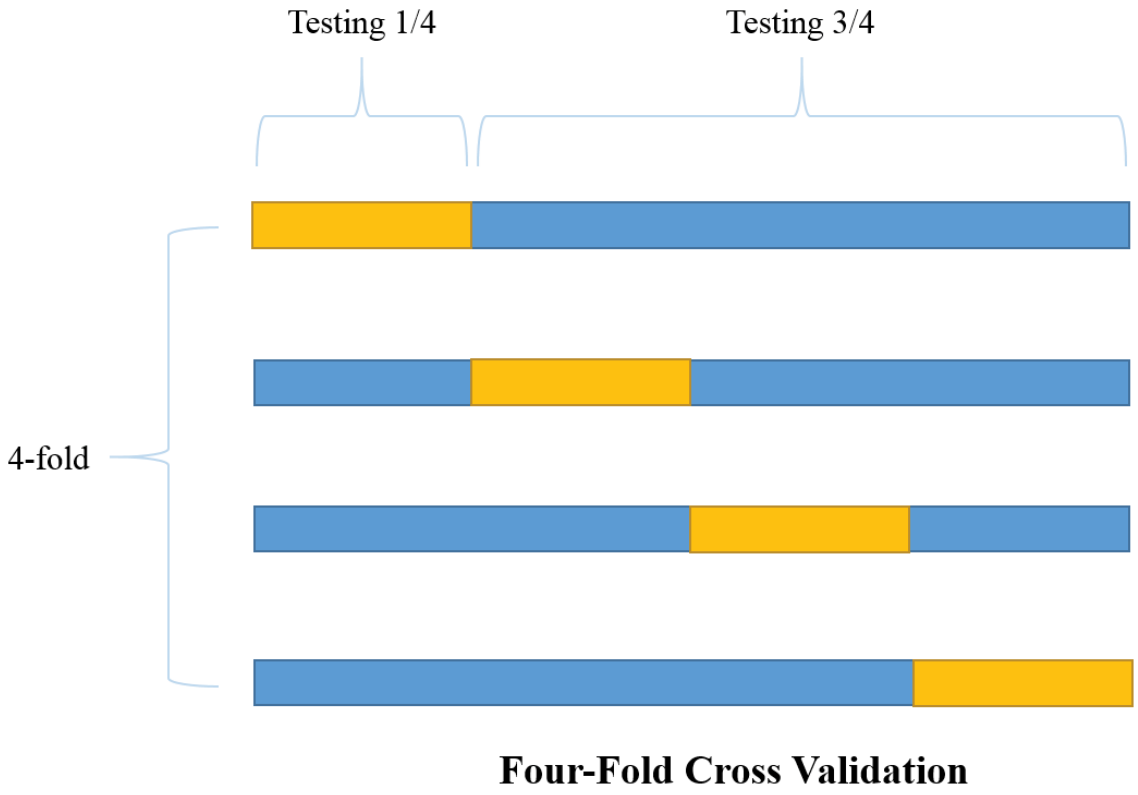

Figure 23: Magnetic dataset in the four-fold cross validation

Firstly, we divided the entire set of experimental data into a testing set and a training set, comprising 1/4 and 3/4 of the entire data respectively. Moreover, we use Dynamic Time Warping (DTW) to select lower value that is in left data as training dataset.

The four results of Experiment are presented in Table 8, 9, 10, and 11.

Table 8: Experiment 1 results: Vehicle classification using 3/4 of measurement data as training data and 1/4 data as testing data for three-dimensional map

	Sedan	VAN	Truck	Bus	Non-vehicle
Observed	53	22	21	20	92
Training data	36	17	15	13	54
Testing data	13	5	5	5	23
Algorithm classification	11	4	4	5	23
Algorithm accuracy	85%	80%	80%	100%	100%

Table 9: Experiment 2 results: Vehicle classification using 3/4 of measurement data as training data and 1/4 data as testing data for three-dimensional map

	Sedan	VAN	Truck	Bus	Non-vehicle
Observed	53	22	21	20	92
Training data	34	14	13	13	64
Testing data	13	5	5	5	23
Algorithm classification	12	5	5	5	21
Algorithm accuracy	92%	100%	100%	100%	91%

Table 80: Experiment 3 results: Vehicle classification using 3/4 of measurement data as training data and 1/4 data as testing data for three-dimensional map

	Sedan	VAN	Truck	Bus	Non-vehicle
Observed	53	22	21	20	92
Training data	38	16	14	12	61
Testing data	13	6	5	5	23
Algorithm classification	13	4	5	5	22
Algorithm accuracy	100%	67%	100%	100%	96%

Table 9: Experiment 4 results: Vehicle classification using 3/4 of measurement data as training data and 1/4 data as testing data for three-dimensional map

	Sedan	VAN	Truck	Bus	Non-vehicle
Observed	53	22	21	20	92
Training data	37	15	14	13	59
Testing data	14	6	6	5	23
Algorithm classification	13	5	5	5	23
Algorithm accuracy	93%	83%	83%	100%	100%

6.3 Impact on experimental accuracy

According to the experimental results for the one- and three-dimensional maps, we can conclude that the different models have different results, while increasing training data can improve experimental accuracy. However, selecting raw magnetic signals can also

improve accuracy to a significant extent. DTW as a filter makes a great contribution to increasing experimental accuracy for the three-dimensional map. Therefore, the selection of training accuracy is crucial for experimental accuracy. In literature review, Saowaluck et al. [51] and Zhou and Wang [74] have achieved the overall accuracy, which is 81.69% and 84% respectively. Compared with their accuracy, we can achieve 94% on average.

Chapter 7: Conclusion and future work

7.1 Conclusion

In this dissertation, we present a road vehicle identification and classification approach using magnetic sensor and magnetic signal feature extraction and classification, as well as data processing. This approach is designed for analysing road traffic in intelligent transportation systems. Using this approach, the installation of a magnetic sensor at the roadside does not require interruption of road traffic; this reduces deployment and maintenance costs. The raw magnetic measurement signal is filtered by DTW, and the processing approach extends MFCC to extract the magnetic signal features and classify these features to categorise five types of vehicle signals. Using this approach, the average accuracy of vehicle classification reached in our test data is: Sedan 92%, Van 86%, Truck 90%, Bus 100%, and Non-Vehicle 97%. In general, the average accuracy in our all test data is over 90%.

7.2 Open research issues

Although a comprehensive empirical study has been presented and a high level of recognition accuracy has been achieved, there are currently only four vehicles types in our research (i.e. sedan, van, truck and bus). We need to expand the categories of vehicle types and increase the accuracy of classification.

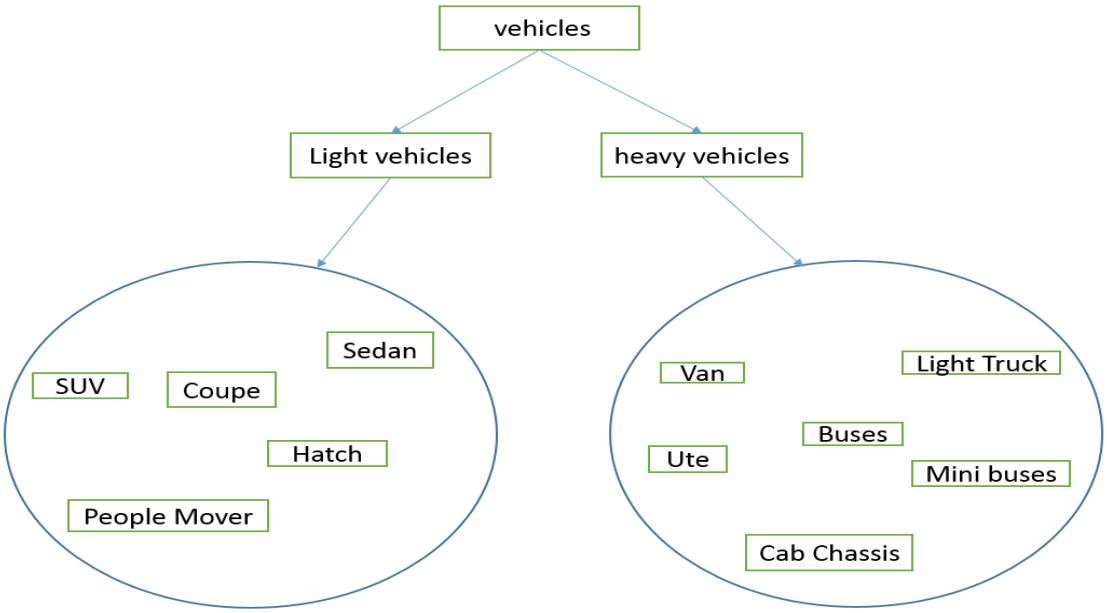

Figure 24: New vehicle classification

In our future work, we will aim to improve both the vehicle data and the classification accuracy by exploring new algorithms. In Figure 24, we increase the data to 3000, including SUV, Coupe, Sedan, People-Mover, Hatch, Van, Ute, Buses, Cab Chassis, Mini-Bus, Light Truck, and Light Bus. Moreover, the toughest challenge in our measurements is the case of more than two vehicles in complex road traffic; when there are four or five different vehicles passing the sensor, we need to recognise them simultaneously. We will further consider the dependence of accuracy on the number of sensors, the distance between passing vehicles and AMR sensor and other environmental parameters.

Reference

[1] US Department of Transportation (2006) “Federal Highway Administration Research and Technology Coordinating, Developing Highway Transportation Innovations” May 2006

[2] Mazarakis Georgios and Avaritsiotis (2007) “Vehicle classification in sensor networks using time-domain signal processing and neural networks”, Microprocessors and MICROSYSTEMS, Vol 31. pp 381-392, Feb. 2007

[3] Yong-Kul Ki and Doo-Kwon Baik (2006) “Vehicle-classification algorithm for single-loop detectors using neural networks”, IEEE Trans. On Vehicle Technology, Vol. 55, No. 6, pp 1704-1711, Nov. 2006

[4] L. E. Y. Mimbela, and L. A. Klein. “A summary of vehicle detection and surveillance technologies used in intelligent transportation systems,” The Vehicle Detector Clearinghouse, August 2007.

[5] Bajaj P, Sharma P, and Deshmukh, “Bajaj, Preeti, Prashant Sharma, and Amol Deshmukh.(2007) "Vehicle Classification for Single Loop Detector with Neural Genetic Controller: A Design Approach." Intelligent Transportation Systems Conference, 2007. ITSC 2007. IEEE.

[6] Gajda J. and Stencel M.(2014) “A highly selective vehicle classification utilizing dual-loop inductive detector ”, Metrology and measurement systems, 2014, 21 (3), pp 473-484.

[7] PORTELLI B, GRECH I, CASHA O, et al. Design considerations and optimization for 3-axis anisotropic magneto-resistive sensors[C].Electrotechnical Conference. IEEE, 2016:1-6.

[8] Roe H. and Hobson GS. (1992) “Improved discrimination of microwave vehicle profiles”, IEEE MTT-S International Microwave Symposium Digest 1992, 2:717-720 Vol 2.

[9] MCFEE J E, DAS Y. Determination of the parameters of a dipole by measurement of its magnetic field [J]. IEEE Transactions on Antennas & Propagation, 1981, 29(2):282-287.

[10] Ignacio Llamas-Garro, Konstantin Lukin, Marcos T. de Melo; Jung-Mu Kim, (2016) “Frequency and angular estimation of detected microwave source using aerial vehicles”, 2016 IEEE MTT-S Latin America Microwave Conference (LAMC), Poerto Vallarta, Mexico.

[11] S. Matzka and R. Altendorfer, “A comparison of track-to-track fusion algorithms for automotive sensor fusion,” in Proc. IEEE Int. Conf. Multisensor Fusion Integr. Intell. Syst., Seoul, Korea, Aug. 20–22, 2008, pp. 189–194.

[12] B. Cifman, S. Krishnamurthy, Vehicle reidentification and travel time measurement across freeway junctions using the existing detector infrastructure. In Transportation Research Part C: Emerging Technologies, vol. 15, no. 3, pp. 135-153, June 2007.

[13] T. Lefebvre, H. Bruyninckx, and J. De Schuller, "Comment on 'A new method for the nonlinear transformation of means and covariances in filters and estimators' [and authors' reply]," IEEE Trans. Autom. Control, vol. 47, no. 8, pp. 1406–1409, Aug. 2002.

[14] Hurney Patrick, Waidron Peter, Morgan Fearghal, Jone Edward, Glavin Martin (2015) "Night-time pedestrian classification with histograms of oriented gradients-local binary patterns vectors", IEEE Transactions on Intelligent Transportation Systems. 2015, Vol. 9, Issue 1.

[15] M. S. Shehata, J. Cai, W. M. Badawy, T. W. Burr, M. S. Pervez, R. J. Johannesson, and A. Radmanesh, "Videobased automatic incident detection for smart roads: The outdoor environmental challenges regarding false alarms," IEEE Trans. on Intelligent Transportation Systems, vol. 9, no. 2, pp. 349-360,2008.

[16] S. Coleri, S. Y. Cheung, and P. Varaiya. "Sensor networks for monitoring traffic," Allerton conference on communication, control and computing, 2004, pp. 32-40.

[17] R. R. Cabrera, T. Tuytelaars, and L. van Gool, "Efficient multi-camera vehicle detection, tracking, and identification in a tunnel surveillance application," Computer Vision and Image Understanding, vol. 116, no. 6,pp. 742-753,2012.

[18] X. Wang, "Intelligent multi-camera video surveillance: A review," Pattern Recognition Letters, vol. 34, no. I , pp. 3-19, 2013.

[19] M. J. Caruso and L. S. Withanawasam. "Vehicle detection and compass applications using AMR magnetic sensors," Sensors Expo Proceedings, vol. 477. 1999.

[20] Shi, Shengli, Zhong Qin, and Jianmin Xu (2007) "Robust algorithm of vehicle classification", Software Engineering, Artificial Intelligence, Networking, and Parallel/Distributed Computing, 2007. SNPD 2007. Eighth ACIS International Conference on. Vol. 3. IEEE, 2007.

[21] NARA T, SUZUKI S, ANDO S. A Closed-Form Formula for Magnetic Dipole Localization by Measurement of Its Magnetic Field and Spatial Gradients[J]. IEEE Transactions on Magnetics, 2006, 42(10):3291-3293.

[22] K. Kwong, R. Kavaler, R. Rajagopal, P. Varaiya, Real-Time Measurement of Link Vehicle Count and Travel Time in a Road Network, IEEE Transactions on Intelligent Transport Systems, vol. 11, no. 4, December 2010.

[23] J. Barcelo, L. Montero, L. Marques, C. Carmona, Travel Time Forecasting and Dynamic Origin-Destination Estimation for Freeways Based on Bluetooth Traffic Monitoring. Transportation Research Record, no. 2175, pp. 19-28. 2010.

[24] M. H. Kang, B. W. Choi, K. C. Koh, J. H. Lees, and G. T. Park, "Experimental study of a vehicle detector with an AMR sensor," Sens. Actuators A, Phys., vol. 118, no. 2, pp. 278–284, Feb. 2005.

[25] Chou, Hsi-Tseng & Tuan, Shih-Chung & Ho, Hsien-Kwei. (2016). "Numerical estimation of electromagnetic backscattering from near-zone vehicles for the side-look vehicle-detection radar applications at millimeter waves", IEEE, 129-133. 10.1109.

[26] Y. Tan, F. Han and F. Ibrahim, A Radar Guided Vision System for Vehicle Validation and Vehicle Motion Characterization, in Proceedings of IEEE Intelligent Transportation Systems Conference, 2007: 1059–1066.

[27] X. Liu, Z. Sun and H. He, On-road vehicle detection fusing radar and vision, in Proceedings of IEEE International Conference on Vehicular Electronics and Safety, 2011: 150–154.

[28] X. Wang, L. Xu, H. Sun, J. Xin and N. Zheng, Bionic vision inspired on-road obstacle detection and tracking using radar and visual information, in Proceedings of IEEE Intelligent Transportation Systems Conference, 2014: 39–44.

[29] U. Kadow, G. Schneider, and A. Vukotich, Radar-vision based vehicle recognition with evolutionary optimized and boosted features, in Proceedings of IEEE Symposium on Intelligent Vehicles, 2007: 749–754.

[30] Urazghildiiev, Ildar & Ragnarsson, Rolf & Ridderstrom, Pierre & Rydberg, Anders & Ojefors, Eric & Wallin, Kjell & Enochsson, Per & Ericson, Magnus & Lofqvist, Gran. (2007). "Vehicle Classification Based on the Radar Measurement of Height Profiles. Intelligent Transportation Systems", IEEE Transactions on. 8. 245 - 253. 10.1109.

[31] Y. Bar-Shalom, X. Rong Li, and T. Kirubarajan, Estimation with Applications to Tracking and Navigation. New York: Wiley, 2001.

[32] S. Wender and K. Dietmayer. 3d vehicle detection using a laser scanner and a video camera. IET Intelligent Transport Systems, vol. 2, no. 2, pp. 105-112. 2008.

[33] S. Sivaraman, and M. Trivedi, Looking at Vehicles on the Road: A Survey of Vision-Based Vehicle Detection, Tracking, and Behavior Analysis, IEEE Transactions on Intelligent Transportation Systems, 14(4): 1773–1795, 2013.

[34] Odat, Enas & S. Shamma, Jeff & Claudel, Christian. (2017). “Vehicle Classification and Speed Estimation Using Combined Passive Infrared/Ultrasonic Sensors”, IEEE Transactions on Intelligent Transportation Systems. PP. 1-14. 10.1109.

[35] C. B. da Costa Filho, A & Filho, João & de Araujo, Renato & Augusto Benevides, Clayton. (2009). “Infrared-based system for vehicle classification”, SBMO/IEEE MTT-S International Microwave and Optoelectronics Conference Proceedings. 537-540. 10.1109.

[36] Chen, H.-T & Chu, M.-C & Chou, C.-L & Lee, S.-Y & Lin, B.-S. (2015). “Multi-camera vehicle identification in tunnel surveillance system”, IEEE. 10.1109.

[37] H. W. Kuhn, “The Hungarian method for the assignment problem”, Naval Research Logistics Quarterly, vol. 2, no. 1-2, pp. 83-97, 1955.

[38] G. S. K. Fung, N. H. C. Yung, and G. K. H. Pang. "Vehicle shape approximation from motion for visual traffic surveillance," Proc. IEEE Conf Intell. Transp. Syst., pp. 608-613, August 200l.

[39] R. S. Feris, B. Siddiquie, J. Petterson, Y. Zhai, A. Datta, L. M. Brown, and S. Pankanti, "Large-scale vehicle detection, indexing, and search in urban surveillance videos," IEEE Trans. on Multimedia, vol. 14, no. 1, pp. 28-42, 2012.

[40] Sotheany, Nou & Nuthong, Chaiwat. (2017). “Vehicle classification using neural network”, IEEE, 443-446. 10.1109.

[41] Cai, B.G., Zhao, J.M., Wang, J., et al.: “Design and implementation of vehicle classification based on 3-axis AMR vehicle detector”, J. Transp. Syst. Eng. Inf. Technol., 2014, 14, (4), pp. 46–52.

[42] J. Vcelak, P. Ripka, J. Kubik, A. Platil, and P. Kaspar, “AMR navigation systems and methods of their calibration,” Sens. Actuators A, Phys., vol. 123/124, pp. 122–128, Sep. 23, 2005.

[43] LIU Y, L.X., WANG X, Bias Voltage Correction of HMC1022 AMR Sensor[C].IEEE International Conference on Mechatronics and Automation, 2011:1550-1554.

[44] J.-W. Hsieh, S.-H. Yu, Y.-S. Chen, and W.-F. Hu. “Automatic traffic surveillance system for vehicle tracking and classification," IEEE Trans. Intell. Transp. Syst., vol. 7, no. 2, pp. 175-177, June 2006.

[45] Hunter, T., Abbeel, P., Bayen, A.M.: “The path inference filter: model-based low-latency map matching of probe vehicle data”, Algorithmic Found. Rob. X, Springer Berlin Heidelberg, 2013, pp. 591–607.

[46] Cao, P., Miwa, T., Yamamoto, T., et al.: “Bi-level GLS estimation of dynamic origin-destination matrix for urban network using probe vehicle data”, Transportation Research Board 92nd Annual Meeting, 2013, pp. 13–24.

[47] Zhang, Z., Yang, D., Zhang, T., et al.: “A study on the method for cleaning and repairing the probe vehicle data”, IEEE Trans. Intell. Transp. Syst., 2013, 14, (1), pp. 419–427.

[48] Wang, Hua & Meng, Liu. (2017). “Vehicle Detection Using Three-Axis AMR Sensors Deployed along Travel Lane Markings”. IET Intelligent Transport Systems. 11. . 10.1049.

[49] Z. lei, R. Wang, and L. Cui. “Real-time Traffic Monitoring with Magnetic Sensor Networks,” Journal of information science and engineering, vol. 27(4), 2011, pp. 1473-1486.

[50] Cheung, Sing, et al. (2005) “Traffic measurement and vehicle classification with single magnetic sensor”, Transportation research record: journal of the transportation research board 1917 (2005): 173-181.

[51] Keawkamnerd, Saowaluck, Jatuporn Chinrungrueng, and Chaipat Jaruchart (2008) "Vehicle classification with low computation magnetic sensor", ITS Telecommunications, 2008. ITST 2008. 8th International Conference on. IEEE, 2008.

[52] Taghvaeeym S. and Rajamani R. (2014) “Portable roadside sensors for vehicle counting, classification, and speed measurement”, IEEE Transactions on Intelligent Transportation Systems, Vol. 15, No. 1, 2014.

[53] Yang Bo and Lei Yiqun, (2015) “Vehicle detection and classification for low-speed congested traffic with anisotropic magnetoresistive sensor’, IEEE Sensors Journal, Vol. 15, No. 2, Feb. 2015.

[54] S. Y. Cheung et al., Traffic measurement and vehicle classification with a single magnetic sensor. In Proceedings of the 84th Annual Meeting of the Transportation Research Board, 2005, pp. 173-181.

[55] STOLZ R, Z.V., SCHULZ M, et al, Magnetic full-tensor SQUID gradiometer system for geophysical applications[J].The Leading Edge, 2006. 25(2): 178-180.

[56] NARA T, W.H, ITO W, Divergence form of Euler’s equation for magnetic dipole localization[C].SICE Annual Conference (SICE), 2011 Proceedings of. IEEE, 2011: 2356-2360.

[57] S. Oh, S. G. Ritchie and C. Oh, Real-time traffic measurement from single loop inductive signatures. In Transportation Research Record 1804. Washington, DC: TRB, National Research Council, 2002, pp. 98106

[58] MERLAT L, NAZ P. Magnetic localization and identification of vehicles[J]. Proc Spie, 2003, 5090:174-185.

[59] MCGARY J E. Real-Time Tumor Tracking for Four-Dimensional Computed Tomography Using SQUID Magnetometers[J]. IEEE Transactions on Magnetics, 2009, 45(9):3351-3361.

[60] J. Zhang, F. Y. Wang, K. Wang, W. H. Lin, and C. Chen, "Data-driven intelligent transportation systems: A survey," IEEE Trans. on Intelligent Transportation Systems, vol. 12, no. 4, pp. 1624-1639,20.

[61] FOLEY C P, TILBROOK D L, LESLIE K E, et al. Geophysical exploration using magnetic gradiometry based on HTS SQUIDs[J]. IEEE Transactions on Applied Superconductivity, 2001, 11(1):1375-1378.

[62] A. B. Kandali, A. Routray, and T. K. Basu, (2008) "Emotion recognition from assamese speeches using mfcc features and gmm classifier," in TENCON 2008-2008 IEEE Region 10 Conference. IEEE, 2008, pp. 1–5.

[63] T. F. Quatieri (2002) Discrete-time speech signal processing: principles and practice. Pearson Education India, 2002.

[64] S. E. Bou-Ghazale and J. H. L. Hansen, "A comparative study of traditional and newly proposed features for recognition of speech under stress," IEEE Trans. Speech Audio Process., vol. 8, no. 4, pp. 429–442, Jul. 2000.

[65] S. Singh, and E. Rajan (2011) "Vector Quantization approach for speaker recognition using MFCC and inverted MFCC", International Journal of Computer Applications, Vol. 17, No. 1, Mar 2011.

[66] Gray, Robert. (1984) "Vector quantization." IEEE ASSP Magazine 1.2 (1984): 4-29.

[67] O. Gietelink, J. Ploeg, B. De Schutter, and M. Verhaegen, "Development of ADAS with vehicle HiL simulations," Vehicle System Dynamics, vol. 44, no. 7, pp. 569–590, July 2006.

[68] Zezhi, C., et al. Road vehicle classification using Support Vector Machines. In IEEE International Conference on Intelligent Computing and Intelligent Systems, 2009.

[69] M. Stocker, P. Silvonen, M. Rönkkö, and M. Kolehmainen, "Detection and classification of vehicles by measurement of road-pavement vibration and by means of supervised machine learning," Journal of Intelligent Transportation Systems, vol. 0, 2015

[70] K. Urahama and Y. Furukawa, Gradient descent learning of nearest neighbor classifiers with outlier rejection, Pattern Recognition, vol. 28, no.5, pp. 761-768, 1995.

[71] T.M. Martinetz, S.G. Berkovich and K.J. Schulten, 'Neural-gas' network for vector quantization and its application to time-series prediction, IEEE Trans. Neural Networks, vol.4, pp.558-568, 1993.

[72] Xu L, Ke M. Research on isolated word recognition with DTW based[C]//Computer Science & Education (ICCSE), 2012 7th International Conference on. IEEE, 2012: 139-141.

[73] Yuxin Z, Miyanaga Y. An improved dynamic time warping algorithm employing nonlinear median filtering[C]//Communications and Information Technologies (ISCIT), 2011 11th International Symposium on. IEEE, 2011: 439-442.

[74] Feng, Z., & Mingzhe, W. (2009). A New SVM Algorithm and AMR Sensor Based Vehicle Classification. 2009 Second International Conference on Intelligent Computation Technology and Automation. doi:10.1109/icicta.2009.337

List of research publications

[1] B. Zhang, J. Zhao, **X. Chen** & J. Wu, 'ECG data compression using a neural network model based on multi-objective optimization', *PLoS ONE*, https://doi.org/10.1371/journal.pone.0182500, 2017.

[2] **X. Chen**, X. Kong & M. Xu, 'Road Vehicle Recognition Using Magnetic Sensing Feature Extraction and Classification'. View/Download from: UTS OPUS, 2018.

[3] **X. Chen**, X. Kong & M. Xu, 'Road Vehicle Detection and Classification Using Magnetic Field Measurement and 3-Dimensional Discrete Element Method', submitted to IEEE ACCESS